Online digital archive of aerial photographs (1935–1941) of Ethiopia

Jan Nyssen, Martijn Debever, Gezahegne Gebremeskel, Bart de Wit, Kiros Meles Hadgu, Steven de Vriese, Jeffrey Verbeurgt, Amaury Frankl, Tulu Besha, Jan Kropáček, et al.

▶ **To cite this version:**

Jan Nyssen, Martijn Debever, Gezahegne Gebremeskel, Bart de Wit, Kiros Meles Hadgu, et al.. Online digital archive of aerial photographs (1935–1941) of Ethiopia. Geoscience Data Journal, In press, 34 p. 10.1002/gdj3.115 . hal-03340867

HAL Id: hal-03340867
https://hal.inrae.fr/hal-03340867

Submitted on 18 May 2022

Received: 21 November 2020 | Revised: 8 January 2021 | Accepted: 10 February 2021

DOI: 10.1002/gdj3.115

DATA PAPER

Geoscience Data Journal RMetS WILEY

Online digital archive of aerial photographs (1935–1941) of Ethiopia

Jan Nyssen[1] | Martijn Debever[1] | Gezahegne Gebremeskel[2] | Bart De Wit[1] | Kiros Meles Hadgu[3,4] | Steven De Vriese[1] | Jeffrey Verbeurgt[1] | Amaury Frankl[1,5] | Tulu Besha[2] | Jan Kropáček[6] | Astrid Forceville[1] | Biadgilgn Demissie[3,7]

[1]Department of Geography, Ghent University, Gent, Belgium

[2]Ethiopian Geospatial Information Institute, Addis Ababa, Ethiopia

[3]Institute of Geoinformation and Earth Observation Sciences, Mekelle University, Mekelle, Ethiopia

[4]World Agroforestry (ICRAF) - Ethiopia, Addis Ababa, Ethiopia

[5]INRAE, AMAP, IRD, CIRAD, CNRS, University Montpellier, Montpellier, France

[6]Department of Physical Geography and Geoecology, Charles University, Prague, Czech Republic

[7]Department of Geography and Environmental Studies, Mekelle University, Mekelle, Ethiopia

Correspondence
Jan Nyssen, Department of Geography, Ghent University, Krijgslaan 281 (S8), B-9000 Gent, Belgium.
Email: jan.nyssen@ugent.be

Abstract

The archive of aerial photographs, dating 1935–1941 and covering parts of north and central of Ethiopia, is one of the few archives with pre-1960 remotely sensed data in Africa. It allows adding 30 years of time depth for geographical studies, in contrast to the commonly known oldest imagery dating to 1964, sometimes 1958. These photographs were originally acquired by the Italian military forces, to obtain raw material for warfare purposes and the production of topographic maps. To make the archive accessible, it has been scanned and georeferenced. Procedures used in georeferencing and digitally archiving are detailed in this paper, as well as our experiences with orthorectification and use of the photosets in scientific research. This data set of aerial photographs of Ethiopia in the 1930s has been availed to the wider scientific community through the Pangaea website http://doi.org/10.1594/PANGAEA.920077 (Nyssen *et al*., 2020, *Aerial photographs of Ethiopia 1935–1941*) Additionally, a web interface (http://www.ethiopia1935.ugent.be/) allows scientists visualizing the location of relocated photographs, and to select and freely order scenes of interest.

KEYWORDS

Ethiopia, historical aerial photographs, Italy, orthorectification, remote sensing

Dataset details

Dataset Identifier: https://doi.org/10.1594/PANGAEA.920077; http://www.ethiopia1935.ugent.be/

Creator: Jan Nyssen, Martijn Debever, Gezahegne Gebremeskel, Bart De Wit, Kiros Meles Hadgu, Steven De Vriese, Jeffrey Verbeurgt, Sultan Mohammed, Amaury Frankl, Tulu Besha, Jan Kropácek, Astrid Forceville, Biadgilgn Demissie

Dataset correspondence: jan.nyssen@ugent.be

Title: Aerial photographs of Ethiopia 1935-1941

Publisher: Pangaea; UGent

Publication year: 2020

Resource type: Data set

Version: 20210310

1 | BACKGROUND & SUMMARY

There are few publications concerning digital archives of historical aerial photographs, mostly regarding the USA, particularly California in 1938 (Ma, 2013), Illinois in the 1930s (Luman *et al*., 1997), the Everglades in the 1920s (Smith *et al*., 2010) or the overall USA (McAuliffe *et al*., 2017), and rarely from Europe such as Wales (Wilson *et al*., 2016). Very few stress the need for user-friendly digital archives or online interface (Caswell, 2012; Long *et al*., 2005; Mathews, 2005). In addition to the earlier listed historical imagery (Nyssen *et al*., 2016), millions of analogue historical aerial photographs covering parts of Africa (sometimes dating back to the 1920s) are dispersed in archives, among others in Zimbabwe (Whitlow, 1988), France (Michel, 2018), U.K., Uganda, Tanzania and Kenya (Kuns, 2010), and Zambia (Pullan, 1976). Yet, few digital archives of aerial photographs are available for the African continent (Table 1).

For Ethiopia, an archive of aerial photographs (APs), dating 1935–1941 and covering large parts of the northern and central parts of the country, is available. It allows adding 30 years of time depth for geographical studies, in contrast to the commonly known oldest APs dating mainly to 1964 and 1986, sometimes to 1958. The APs of the 1930s were originally acquired by the Italian military forces, mostly by the 7th *Topocartographic Section* of the *Istituto Geografico Militare* (IGM), to obtain raw material for warfare purposes and the production of topographic maps during Italian occupation. The archive consists of approximately of 34 000 APs, taken along 94 different flight lines. These APs are of great value for environmental and historical studies about the area they are covering, such as changes in land cover, hydrology or geomorphology. In the next step, these photographs have been digitally availed to Ethiopian universities, research institutes and to the broader scientific community.

In this paper, we discuss the data set and its processing as well as procedures followed to semi-automatically avail it to end users. State-of-the-art information is also presented on ways to process and analyse subsets of the AP collection.

2 | METHODS: REALIZATION OF THE AERIAL PHOTOGRAPHS

2.1 | Equipment

For the purpose of mapping in Libya and East Africa, where a wide angular coverage of large areas of terrain in a single set of exposures was required for small-scale mapping, a four-coupled version of Santoni's Model II camera (Gentilli, 1992; Traversi, 1964) was developed. The original Model II twin camera unit was equipped with two lenses, with each lens having a focal length of 175 mm. The twin cameras used photographic glass plates to record the resulting images in two separate focal planes, with each negative image being 10 × 15 cm in size. Each of the two rotating cylindrical drum magazines held 200 of such glass plates (IGM, 1939). The four-coupled version comprised two of the twin camera units coupled together in such a way that each angle between successive lenses was 30°, which led to coverage with a consistent geometry (IGM, 1939).

The four-camera unit could be oscillated around its horizontal axis between successive sets of exposures, thus allowing the exposure of the high-oblique photographs alternately to the left and right of the flight line. The high-oblique photographs nearly do not overlap, due to their alternating left and right position. The wide image coverage allowed flying at lower altitudes (IGM, 1939). Obviously, this has led to large geometric distortions, a problem that was considered as secondary to the high precision of the photographs (Bergaglio, 2001).

2.2 | Flights and photography

The data acquisition was executed by the 7th Topocartographic Section of IGM. A three-engined, high-wing Caproni Ca-101 D2 aircraft and a crew were provided by the Italian Royal Air Force (Regia Aeronautica) to undertake the flying of the aerial photographic coverage (IGM, 1939). Flights were operated systematically, combining both direct military needs and the preparation of topographic map sheets (Bergaglio, 2001). However, there were neither available flight coordinates nor regular flight patterns (Nyssen *et al*., 2016).

Flights were reportedly planned to have an approximate overlap of 60% between subsequent sets of APs to ensure stereo-coverage of the terrain to use them for stereographic restitution (IGM, 1939). Overlapping areas were calculated in ArcGIS on five subsets of subsequent APs taken over Tembien (Debever, 2019) using Honeycutt's '*spaghetti and meatball*' Count Overlapping Polygons method (Taylor, 2019).

The lack of overlapping areas for subsequent APs within one flight line varies between 5% and 28% for the vertical APs (also referred to as 'frames') and between 8% and 22% for the low-oblique frames. In some flights, overlap decreased as the flight progressed, probably flight velocity was increased as clouds were building through the day (Debever, 2019). Flights over Tembien were dense in relation to Italian military needs for the Battles of Tembien (Barker, 1968). Yet, the area has not been fully covered by vertical and low-oblique frames (Figure 1). When including the high-oblique frames, the coverage is much better (Debever, 2019). Such bird's eye views can however only be used for qualitative analysis (Figure 2).

3 | DATA RECORDS

3.1 | Original photographs

The original photographs were organized as assemblages consisting of a label with metadata and four photographs – one nadir-pointing, two low-oblique (28°30′ to the nadir)

TABLE 1 Digital archives of pre-1960 aerial photographs of Africa

Country	Period	Type of online database	Online ordering and delivery	Web address	Number of APs	Reference
Sudan, Egypt	1920–1959	Not georeferenced	N	https://www.dur.ac.uk/library/asc/sudan/	Approx. 20	Durham University (2020)
Africa, various	1920–1959	Georeferenced, search by coordinates	N	https://www.archives.gov/research/guide-fed-records/groups/057.html	Unknown	National Archives (2020)
D.R. Congo	1947–1959	Georeferenced	N	http://www.drcmining.org/en/index_html	27,100	DRC Mining (2012)
Africa, Mainly East Africa	1920–1959	Not georeferenced	Y	www.iwm.ac.uk	Approx. 50	IWM (2020)
Sudan, Darfur	1952	Georeferenced	Y	www.wossac.com	44 × 4	WOSSAC (2020)
Sudan, White and Blue Nile Regions	1952–3	Georeferenced	Y	www.wossac.com	N/A	WOSSAC (2020)
Ethiopia	1935–1941	Georeferenced, web interface	Y	http://www.ethiopia1935.ugent.be/	3,132 × 4	Nyssen *et al.* (2020)
Egypt, Sudan, South Sudan, Kenya, Tanzania	1942–1955	Georeferenced, web interface	Y	https://ncap.org.uk	3,478	NCAP (2020)
South Africa	1938–1959	Georeferenced, web interface	Y	http://www.cdngiportal.co.za/cdngiportal/	Many thousands	NGI (2020)

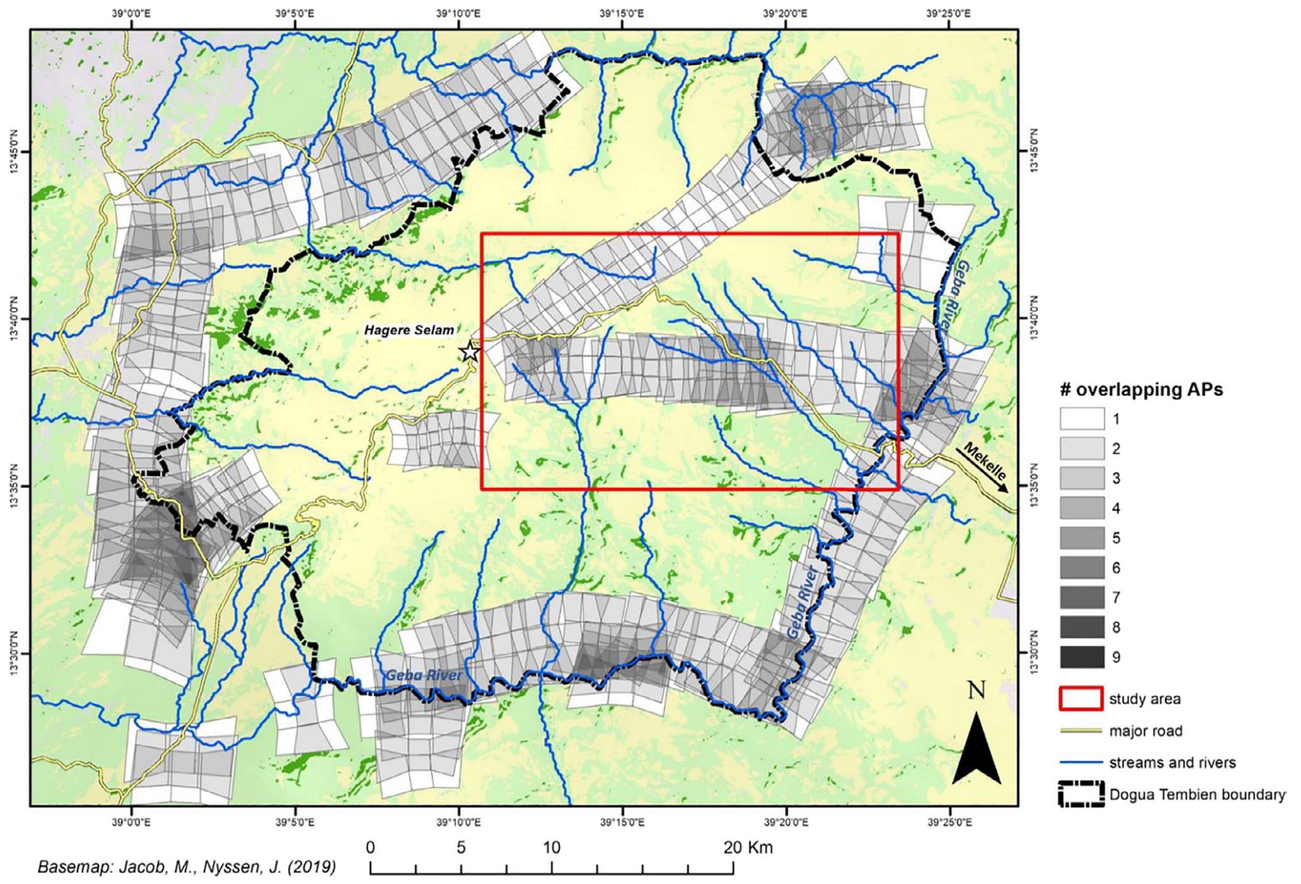

FIGURE 1 Example of ground coverage and overlapping areas for the vertical and low-oblique frames of 1935–36 taken above Dogu'a Tembien. Red rectangle shows area represented in Figure 8. Base map: Jacob and Nyssen (2019)

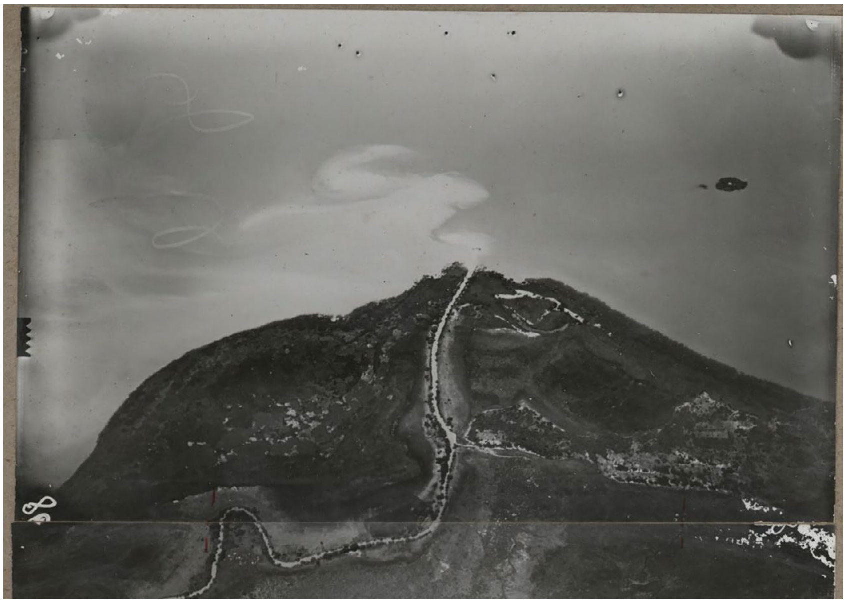

FIGURE 2 High-oblique aerial photograph of the mouth of Gelda River in Lake Tana (11.731126°N, 37.436163°E) in 1938. The view is towards the west. Part of Photoset No. 19381001-86-BaharDar-86-3-100 (Nyssen *et al*., 2020), this bird's eye view is suited for qualitative interpretation: as compared to the 2020 conditions, the delta was much less developed in 1938; the 'cloud' in the lake is a sediment plume

and one high-oblique photograph (57° to the nadir) – glued on 50 × 20 cm hardboard tiles (Figure 3). The frames were cropped manually before gluing, to facilitate the contemporary interpretation of the photosets. The label, present on each assemblage, mentioned at least (1) the flight date of the photoset and (2) a few locations or landmarks covered by the flight (Figure 4). The scale of the APs varies for the vertical frames around 1:12,000 and 1:14,000, and for the oblique frames (valid at their central point) between 1:15,000 and 1:26,000 (Frankl *et al*., 2015a).

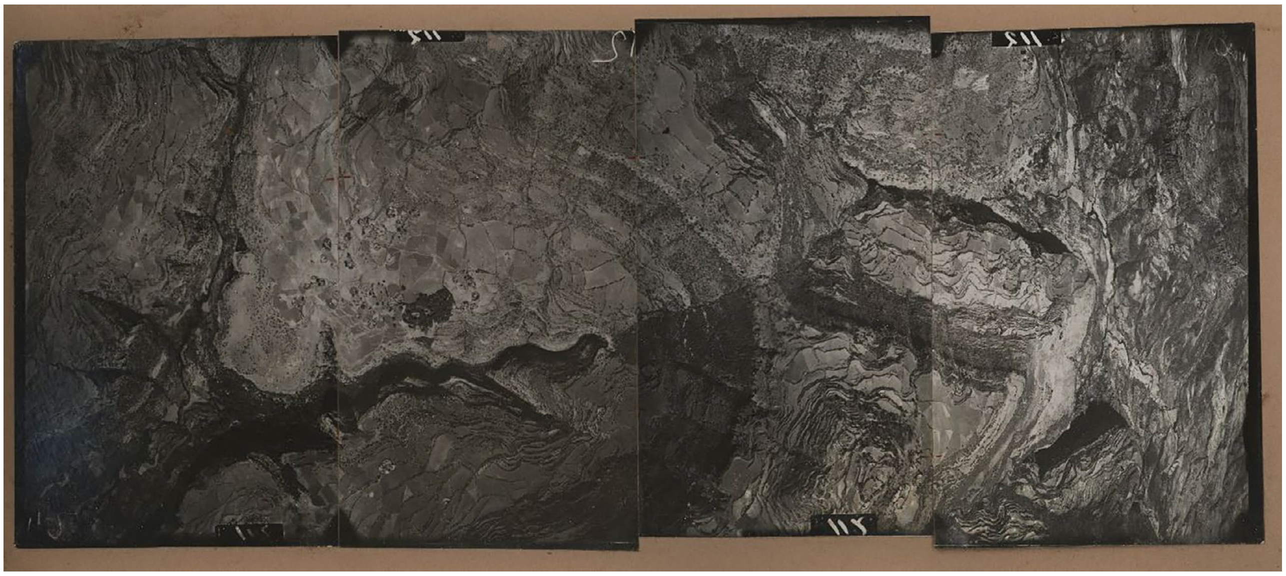

FIGURE 3 Photoset No. 19351231-112-Raio Semaiata-112-97-129 (Nyssen *et al*., 2020), centred on May Tsa'ida (14.14865°N, 39.21475°E). The photograph was taken on 31 December 1935; the code further mentions that this is photoset No. 112, belonging to a series numbered from 97 to 129. 'Raio Semaiata' points to the name that appears on the photograph label, the Italian transliteration of a location in the surroundings

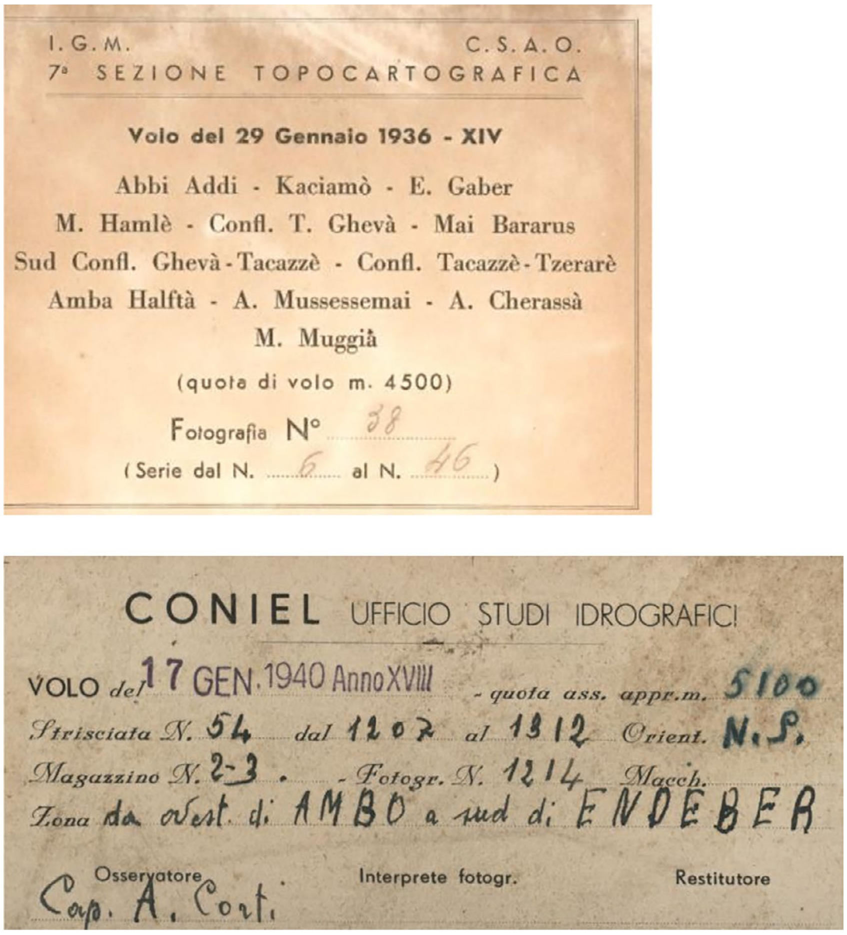

I. G. M. C. S. A. O.
7ª SEZIONE TOPOCARTOGRAFICA

Volo del 29 Gennaio 1936 - XIV

Abbi Addi - Kaciamò - E. Gaber
M. Hamlè - Confl. T. Ghevà - Mai Bararus
Sud Confl. Ghevà - Tacazzè - Confl. Tacazzè - Tzerarè
Amba Halftà - A. Mussessemai - A. Cherassà
M. Muggià

(quota di volo m. 4500)

Fotografia N° 38
(Serie dal N. 6 al N. 46)

CONIEL UFFICIO STUDI IDROGRAFICI

VOLO del 17 GEN. 1940 Anno XVIII - quota ass. appr. m. 5100
Strisciata N. 54 dal 1207 al 1312 Orient. N.S.
Magazzino N. 2-3. - Fotogr. N. 1214 Macch.
Zona da ovest di AMBO a sud di ENDEBER

Osservatore Cap. A. Corti Interprete fotogr. Restitutore

FIGURE 4 Two different types of labels with metadata for photosets 19360129-38-Abbi Addi-Kaciamo-38-6-46 and 19400117-1214-Ambo-Endeber-1214-1207-1312 (Nyssen *et al*., 2020). IGM stands for Istituto Geografico Militare, CSAO for Comando Superiore Africa Orientale, CONIEL for Compagnia Nazionale Imprese Elettriche

3.2 | Digitization and data format

As a result of a contract for scientific collaboration between Ghent University (Belgium), the Ethiopian Mapping Agency (EMA) (now the Ethiopian Geospatial Information Institute) and Mekelle University (Ethiopia) (21/2/2012), all the photographs in the archive have been transformed into digital form at the EMA offices in Addis Ababa in 2012 using a

Plustek A3 scanner (Optic Pro A320) with a resolution of 600 spi (samples per inch, a measurement of the image scanner's resolution).

3.3 | Relocation of the aerial photographs

Data of parallel recording of location, bearing and tilt of the APs (IGM, 1939; Schermerhorn, 1970) could not (yet) be recovered (Nyssen *et al*., 2016). Hence, we endeavoured to locate photosets through visualization of current imagery on screen, using rough locations provided on the labels, typical landmarks on some photographs and sequences along flight lines. Though the work was repetitive and time-taking, it allowed a thorough understanding of the data set and landscapes featured. So far, 3,132 photosets of four frames could be relocated this way (Figure 5).

YYYYMMDD – < serial No. > – < Place name mentioned on label > – < serial No. > – < start No. of series > – < end No. of series >. (3)

3.4 | Metadata structure

A major disadvantage for film-based aerial photography is the limited availability of metadata and its inconsistency (Morgan *et al*., 2010). The conditions in which the APs of Ethiopia in the 1930s were realized involve additional disadvantages: glass plate technology, irregular flight lines, no flight plans, recorded coordinates – if any – not transferred to the photographs. Possible identifiers for the photosets were flight date, locations mentioned on the label (Figure 4) and sequential number, between 1 and 200 which was the maximum number of glass plates the rotational magazines could hold (Nyssen *et al*., 2016). As the recovered original APs were not organized by flight line nor date, and made up a volume of approx. 1 m^2, we have chosen to scan them without preliminary manual sorting by flight lines. During the scanning operations, we had not yet a comprehension of the flight schemes and the photographs, thus, received a preliminary identifier consisting of.

< Place name mentioned on label > – < serial No. > – < start No. of series > – < end No. of series > (1)

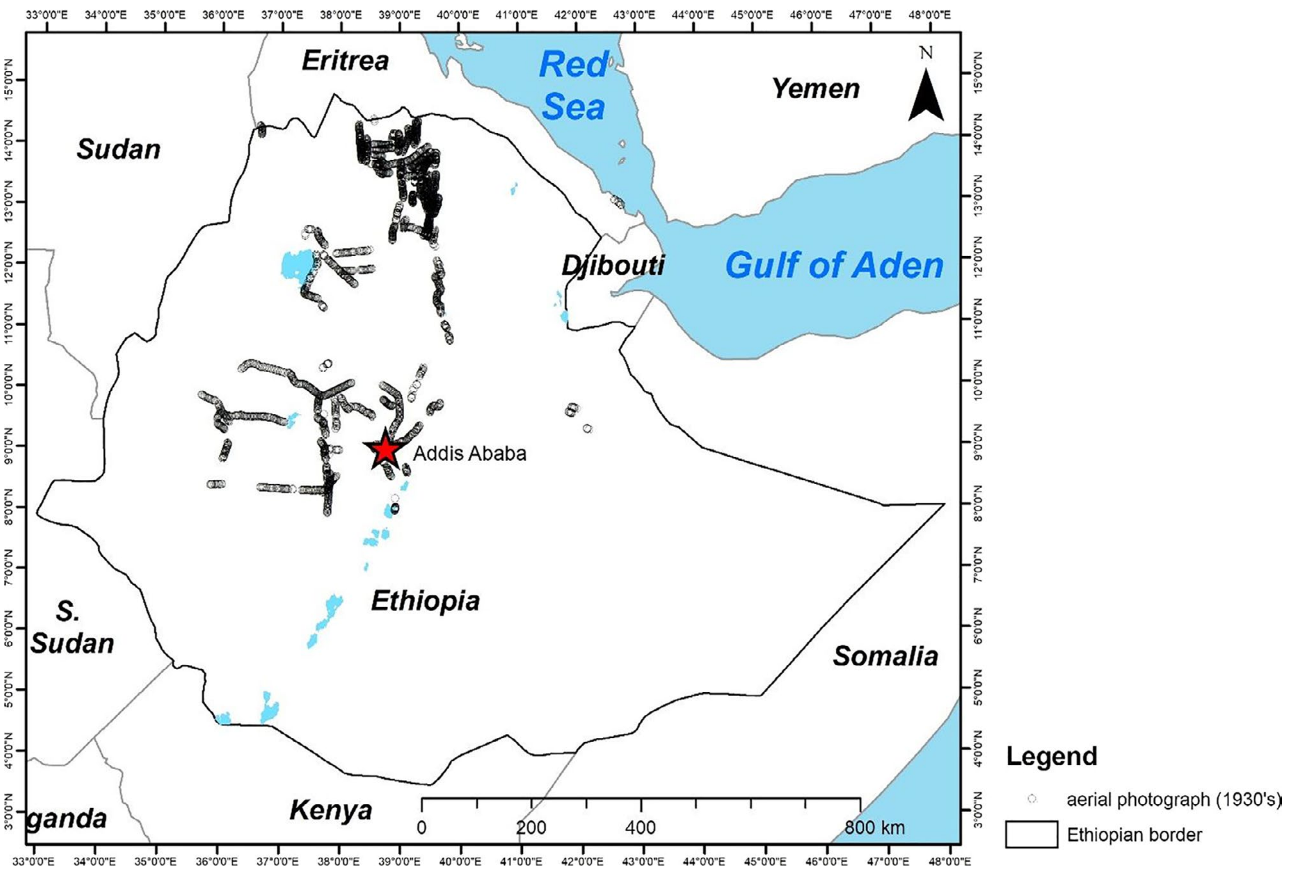

FIGURE 5 Overview of localized APs; 3,132 of the 8,281 tiles, each containing four frames, were localized on 57 different flight lines

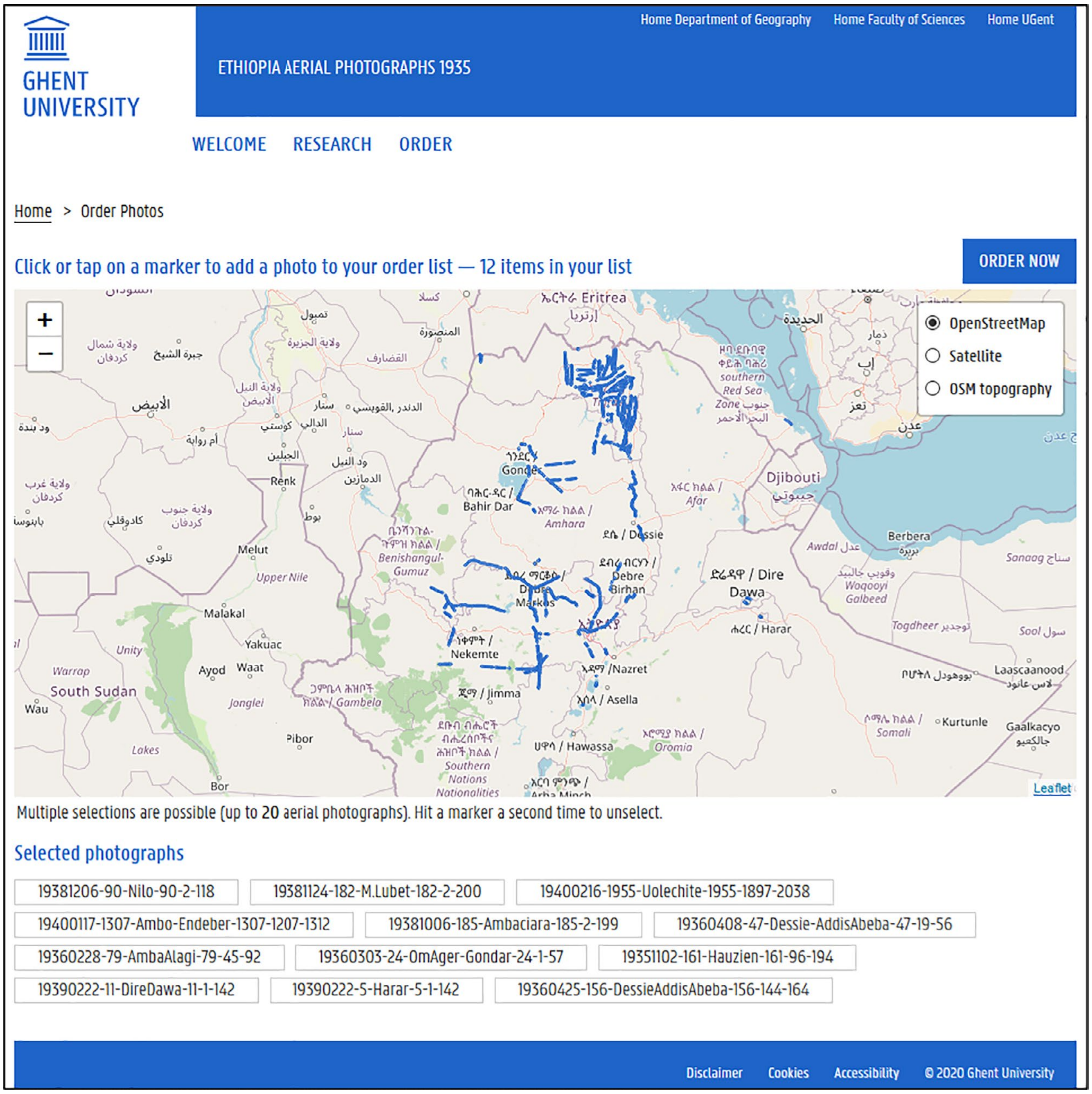

Click or tap on a marker to add a photo to your order list — 12 items in your list

Multiple selections are possible (up to 20 aerial photographs). Hit a marker a second time to unselect.

Selected photographs

19381206-90-Nilo-90-2-118
19381124-182-M.Lubet-182-2-200
19400216-1955-Uolechite-1955-1897-2038
19400117-1307-Ambo-Endeber-1307-1207-1312
19381006-185-Ambaciara-185-2-199
19360408-47-Dessie-AddisAbeba-47-19-56
19360228-79-AmbaAlagi-79-45-92
19360303-24-OmAger-Gondar-24-1-57
19351102-161-Hauzien-161-96-194
19390222-11-DireDawa-11-1-142
19390222-5-Harar-5-1-142
19360425-156-DessieAddisAbeba-156-144-164

FIGURE 6 Online interface to select and order historical APs. Selected APs in this screen-print cover areas in Amhara, Tigray, Benishangul-Gumuz, Oromo, Dire Dawa, Harari, Addis Ababa and Southern regions of Ethiopia and date back to 1935-1940. Base map: ©OSM contributors

Later, the date mentioned on the labels allowed organizing the photosets into folders by date. Fortunately, on most dates, there was only one flight. Only on two dates, there were two flights, one by IGM and the other by the Compagnia Nazionale Imprese Elettriche (*CONIEL*) in the framework of hydropower planning (Massi, 1940; Podestà, 2013), what resulted in corresponding 'bis' folders. For sake of identification, a simple number consisting of.

$$\text{YYYYMMDD} - < \text{serial No.} > \tag{2}$$

was used to allow unequivocally naming the photosets and linking them to coordinates. We have chosen to further maintain the naming given during the scanning stage in order to be able to trace back the photosets in case something would go wrong in renaming. This resulted in:

Label numbers were constructed in the same way, adding '-label' at the end.

Python scripts were developed in order to prepare the scanned photosets for publication on the website. In a first script (Appendix A), all filenames were checked on consistency using regular expressions. Log files were created by the script, indicating the files complying with the file naming proposed in (1) and the files needing manual adaptations to comply with (1). After preparing all files, a second script (Appendix B) was used to automatically list all .TIF files in a directory and its subdirectories. All filenames consistent with (1) were renamed to the structure as given in (3) and converted to .JPG files using settings that reduce the file size to about 10% of the original with nearly no quality loss (~99%). Again, log files were created to indicate possible problematic files or failed conversions. Finally, a third script (Appendix D) was used to read in a .CSV file containing a table of dates, AP numbers and coordinates. Each converted .JPG file was cross-checked with the table and linked to coordinates in case of a matching date and photo number.

The Excel file was exported as CSV, and, using QGIS, transformed into GeoJSON, a format for encoding geographic data structures (Köbben, 2014), that allowed incorporating the AP locations in a Leaflet interface.

3.5 | Online interface

All aerial photographs that could be relocated have been made available to the wider scientific community through a web-based interface. The website is a fully responsive website (Sarabadani Tafreshi *et al*., 2017; Schade, 2014), so that it is also convenient to use on smaller screens like tablets or smartphones. Although possibly less of an issue for an AP serving tool, fully responsive properties are important given that online search engines like Google or Bing have a mobile-first approach in search rankings (Google Search Guides, 2020).

The technology used for creating the website is a mainly Javascript-focused stack, running on a VMWare virtual machine hosted by Ghent University. The backend is a Node.js (OpenJS Foundation, 2020) server protected by an NGINX (F2020 Inc., 2020) webserver (reverse proxy). The Leaflet.js map script (LeafletJS, 2020) in combination with some additional custom functionality (URL encoding, item listing, …) and responsible for the photo selection is written in client side Javascript. In order to stress the project's Ghent University origins, the UGent corporate identity was used to style all pages (Ghent University, 2020).

Because of the email focused nature of this project, a database or database server was not necessary to implement, dramatically improving online security. For automated email communication between the user and the project owners, the third party email service MailJet is used (MailJet, 2020). At present, the free tier is more than sufficient to satisfy all needs. Upgrade to a higher plan is relatively cheap should the need occur in the future.

The web interface (http://www.ethiopia1935.ugent.be/) uses three pages only, with short texts. A first page presents the archive, an overview map with the available photographs, and the project partners (Ghent University, Department of Geography; Mekelle University, Institute of Geoinformation and Earth Observation Sciences (I-GEOS); Ethiopian Geospatial Information Institute). One sample photograph is included at high resolution and downloadable so that the users can see whether this type of APs fits their purpose.

A second page concerns the use of these aerial photographs for research and development. Given the early instrumentation used, the photographs are quite different from classic imagery. Flight lines are not straight, overlap is not always present and the images may be deformed due to their long preservation in poor conditions (Nyssen *et al*., 2016). There is also no systematic coverage of the area. Nevertheless, the photographs have already been used in a dozen of studies. These publications are hyperlinked on the webpage so that potential users can understand possibilities (and drawbacks) before ordering aerial photographs. For sake of copyright, the publications are not directly downloadable, but can be accessed either through the publisher's website, or requested as offprint from the authors.

The third page allows ordering aerial photographs (Figure 6); this is limited to a maximum of 20 photographs, typically the magnitude of locality-based research in Ethiopia. The coverage of the APs is insufficient to think about synoptic use over wide areas. All photosets have been placed as .JPG files on an internal server and can be accessed through a shapefile holding the coordinates of the AP principal points. Using these coordinates, the location of the photosets is visualized through Leaflet, an open-source JavaScript library for interactive maps (https://leafletjs.com). On the map, the area covered by the APs is schematically represented by resizable circular areas, four kilometre across, so that the photoset can be selected by simple clicking. Corresponding script is available as Appendix D.

Visualization of the area of interest is possible as OpenStreetMap© imagery, OSM cycling map (renamed 'OSM topography', which is particularly of use in this mountainous country) and 'Satellite' (which is the ArcGIS online imagery). For the best visualization of the background map, it was chosen not to have names of photos on the map or while hovering over the map. The selection of APs takes place based on their location. Upon pre-selection, the name of the AP appears at the bottom of the map.

While ordering photosets, information is requested on the user and the purpose of the download request. Confirmation of non-commercial use and appropriate literature quotation is mandatory. After selection and approval by the manager, links are transmitted by email allowing a download of the selected photographs from the server.

4 | TECHNICAL VALIDATION: RELIABLE USE OF DATA IN ANALYSIS

4.1 | Map preparation

In the 1930s, in warfare conditions, topographic maps were produced very rapidly from the aerial photographs

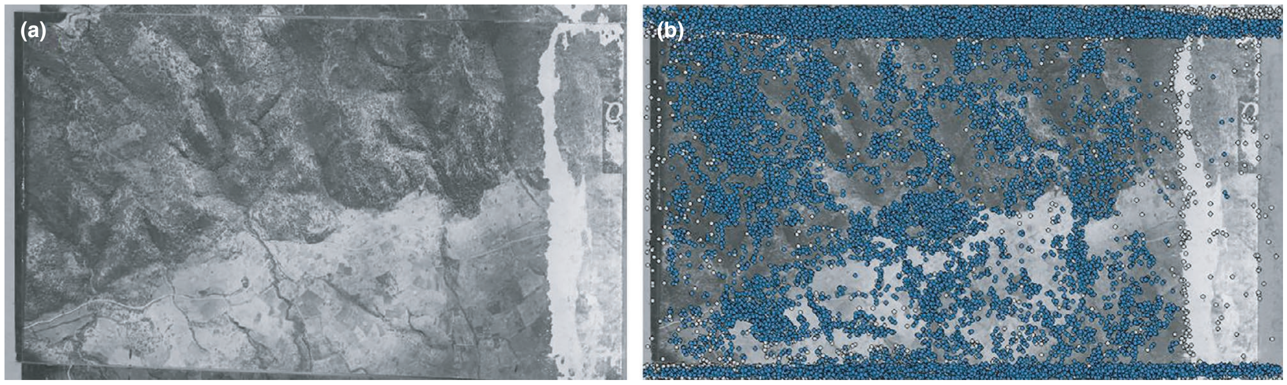

FIGURE 7 A subset of an individual frame in the Kemise graben (19360408-50-Dessie-AddisAbeba-50-19-56) with (a) narrow stripes of adjacent frames and (b) with model covering both the frame and the adjacent stripes

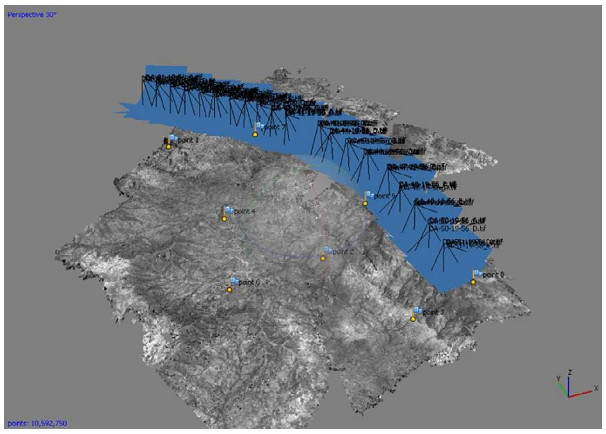

FIGURE 8 Alignment of all frames belonging to photosets 19360408-31-Dessie-AddisAbeba-31-19-56 to 19360408-51 during SfM processing. This PhotoScan model represents the area south of Kombolcha on 8 April 1936

by IGM's 7th Topocartographic Section, a unit that was equipped with extensive photographic, photo-mechanical and printing facilities, located in Asmara (Nyssen *et al*., 2016). These initial maps were mainly planimetric: topographic characteristics were added by rough contour lines to show the relative heights, the shape and the character of the landforms (Nyssen *et al*., 2019). Later on, accurate maps were produced for the same areas at 1:50,000 and 1:100,000 scales (IGM, 1939). The scanned versions are available at the Istituto Geografico Militare Italiano (http://www.igmi.org/ancient/).

4.2 | Qualitative and quantitative studies

A few representative examples of the use of these historical APs include qualitative geomorphic analyses. In the 1930s, the APs were used to study the structural geomorphology of Tigray (Merla & Minucci, 1938) and more recently the long-term dynamics of mountain streams (Ghebreyohannes *et al*., 2015). The APs were also successfully used in a study on historical road engineering geology in the Blue Nile gorge (Hearn, 2019).

Qualitative studies of land cover change (Frankl, 2012; Hishe *et al*., 2020) and land tenure in feudal times (Lanckriet *et al*., 2015; Nyssen & Denaeyer, 2019) have also been carried out using these APs, as well as interpretations of changes to the level of Lake Hayq and urban expansion of Mekelle since the 1930s (Nyssen *et al*., 2016).

Quantitative change studies were carried out using the point-count method (Bellhouse, 1981; Zeimetz *et al*., 1976), hence without orthorectification concerned, particularly in relation to changes in land use (Guyassa *et al*., 2018b) in the Giba basin in Tigray. In the same area, densities of gully and SWC networks were measured by counting the number of features on transversal transect lines (Guyassa *et al*., 2018a).

4.3 | Georeferencing and orthorectification methods and spatially explicit studies

First to third order polynomial transformation using tie points (Hughes *et al*., 2006), also called rubbersheeting or spline, was used to orthorectify the APs and carry out diachronic analysis of land-use changes on the western Rift Valley escarpment (Ghebreyohannes *et al*., 2018), north of Dessie (Kassa *et al*., 2011), around church forests (Scull *et al*., 2017) and at Mt. Guna's treeline (Jacob, 2015). Landsliding was investigated in Dessie, using APs that were processed in the same way (Kropáček *et al*., 2019).

A further step has been the reconstruction of ortho-mosaics and preparation of 3D models of the historical landscapes. We built upon the combination of Structure-from-Motion (SfM) and MultiView Stereo (MVS) (Frankl *et al*., 2015b; James & Robson, 2012) to construct ortho-mosaics and 3D models from aerial photographs. The SfM part makes it possible to reconstruct an area based on an unordered collection of images. By detecting and matching textures in the photographs, they can be matched to each other. The algorithms calculate the camera parameters and the orientation of every picture. Particularly, SfM allows reconstructing the three-dimensional scene geometry and the position of the cameras during the image acquisition period of the images captured around a scene or a landscape, even when imagery is already degraded or when the imagery lacks calibration information (Sevara *et al*., 2018). SfM allows this without using prior topographic data (Peterson, 2017).

To execute the process of SfM-MVS, the most common software PhotoScan, distributed by Agisoft, was used, which extends SfM with MVS. The method was successfully applied in small areas in Tigray (Frankl *et al*., 2015a) and in the Lake Tana basin (Frankl *et al*., 2019), using vertical and low-oblique frames, all manually cropped to single images.

The method was further developed for wider areas. The scanned photosets do not only contain the *scene of interest* (SOI), but are assemblages of four frames. The photographs each contain black borders; strips of the hardboard on which the photographs are glued are also visible on the scans. The scanned photosets were automatically cropped, divided into the individual frames (Appendix E) and contrast stretched using *python* scripts allowing batch processing. As the frames had been cropped before gluing on hardboard, there is no overlap between the vertical and low-oblique APs within the photosets, hence a lack of tie points between the frames which can hinder the correct alignment of the APs in a single geometrical model in the SfM processing. To overcome this problem, the subsets are slightly larger than the AP frames to include also a narrow stripe of the adjacent APs which served as a 'false overlap'. This results in a number of model points in the overlaps between the AP from the same photoset (Figure 7). This approach improved the alignment of the APs but as a drawback it may lead to a lower geometrical accuracy of the model resulting in the occurrence of irregular shapes and gaps in the resulting ortho-mosaic (Forceville, 2018).

A dense point cloud was then built, using the calculated camera positions from the alignment step, from which it calculated depth information for each camera location. Through combination, a single dense point cloud was obtained (Figure 8), which was used as a more detailed and accurate input for the generation of Meshes, Digital Elevation Model (DEM) and the Tiled Model (Agisoft, 2018).

For the construction of a dense point cloud, we set the 'quality' to Ultra High, meaning that the processing was carried out with the original resolution of the photographs. Lower quality parameters result in processing results based on downscaled image sizes. The 'Depth filtering mode' was set to Aggressive for each time period (Debever, 2019), as recommended by *Agisoft PhotoScan*.

Next, a polygonal model – a so-called mesh – was generated, which served as final input for the generation of the ortho-mosaics. As we processed the frames, the mesh processing parameter 'surface type' was set to 'Height field'. The necessary camera parameters (Seitz *et al*., 2006) were computed through SfM, and a spatial resolution of 0.50 m was achieved.

Although *Agisoft Photoscan* offers the possibility to georeference the ortho-mosaics during the process of ortho-mosaicking by adding ground control points (GCPs) after the alignment step, the option of georeferencing the ortho-mosaics in *ArcMAP* was preferred. An investigation of the optimal number of GCPs to be added to the mosaicking process in *Agisoft Photoscan* showed that with an increasing amount of GCPs, the RMSE in X and Y stagnated to an error of approximately 30 m.

As the bearing and tilt information could, unfortunately, not yet be recovered and besides this, the scanners that were used for the scanning operations of the APs could not be calibrated in order to minimize distortions caused by the scanner (Nyssen *et al*., 2016), a spline transformation was used to georeference the ortho-mosaics using numerous GCPs (www.pro.arcgis.com).

On a sample data set, the accuracy was measured by calculating the difference between the X-coordinates (dX) and the Y-coordinates (dY) from a checkpoint on the georeferenced data set – this is a point on the data set that was not used as GCP – and its equivalent in the current landscape. The checkpoints were chosen by means of a regular grid with 1,500 m between nodes. An estimation of the error in X and Y was then interpolated by means of the *kernel density* tool in *ArcMAP*. Errors in the data sets 1935–36 were less than 30 m in *Y* and less than 15 m in *X* (Figure 9) (Debever, 2019).

Errors could be related to the non-uniform scale and geometry of the photographs (particularly for the low-oblique frames in mountain areas) or to random errors during the localization of ground control points. None of the georeferenced data sets show high systematic errors, but some areas have a clearly higher error than the others. The extent of the ortho-mosaics was determined by the quality of the scanned aerial photographs and the number of overlapping APs (Figure 10). Poor quality of some frames is for instance related to local differences in contrast, moisture-induced damage of photographs or presence of clouds. An alternative approach could be to work with less GCPs, generate an error map and then add GCPs in the areas with greatest errors (Persia *et al*., 2020).

Manually cropped subsets, without creating false overlaps, have generally good orthophotographs with only occasionally an artefact or a gap. However, because of a lack of overlap between the vertical photographs and their adjacent low-oblique photographs, in most cases only one camera line is matched.

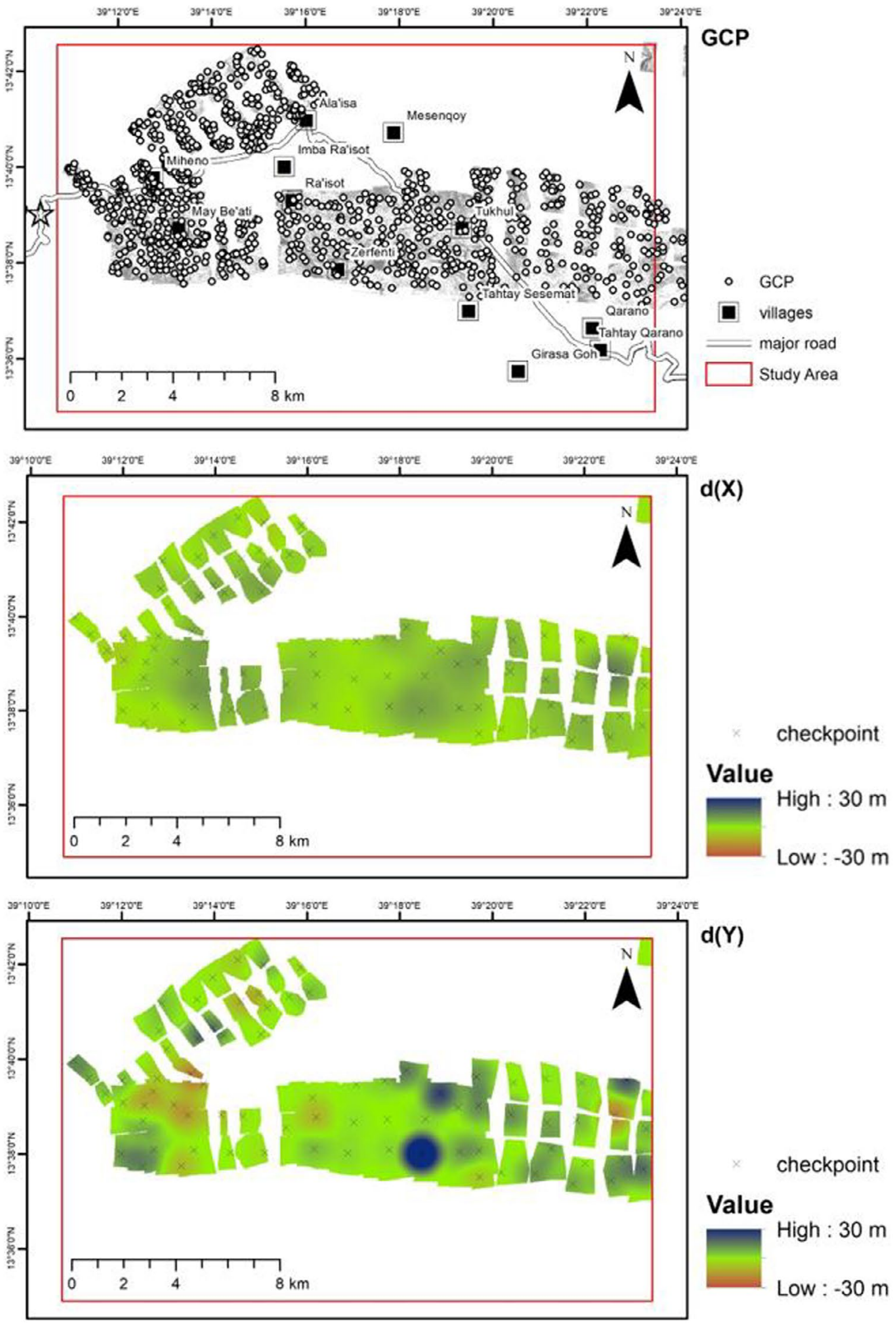

FIGURE 9 Interpolation of checkpoint errors (in meters) for a set of georeferenced ortho-mosaics of 1935–36 in Dogu'a Tembien

When the automatically cropped aerial photographs were processed in PhotoScan, they had a clearly different output. First of all, there were significantly more photographs matched. This is due to the false overlap between low-oblique and vertical photographs. Many of the resulting orthophotographs have however irregular shapes and gaps, and brown lines, parts of the hardboard tiles on which the photographs were glued, appearing between photographs along the flight line. Rather than processing all photographs of one flight line with the same parameters, they would need to be visually inspected and grouped, so that cropping occurs with adjusted parameters (Forceville, 2018). Recent expertise indicates that the implementation of GCPs and terrain heights (Pinto *et al.*, 2019) could help in the orthorectification, while taking into account incomplete metadata (James *et al.*, 2019).

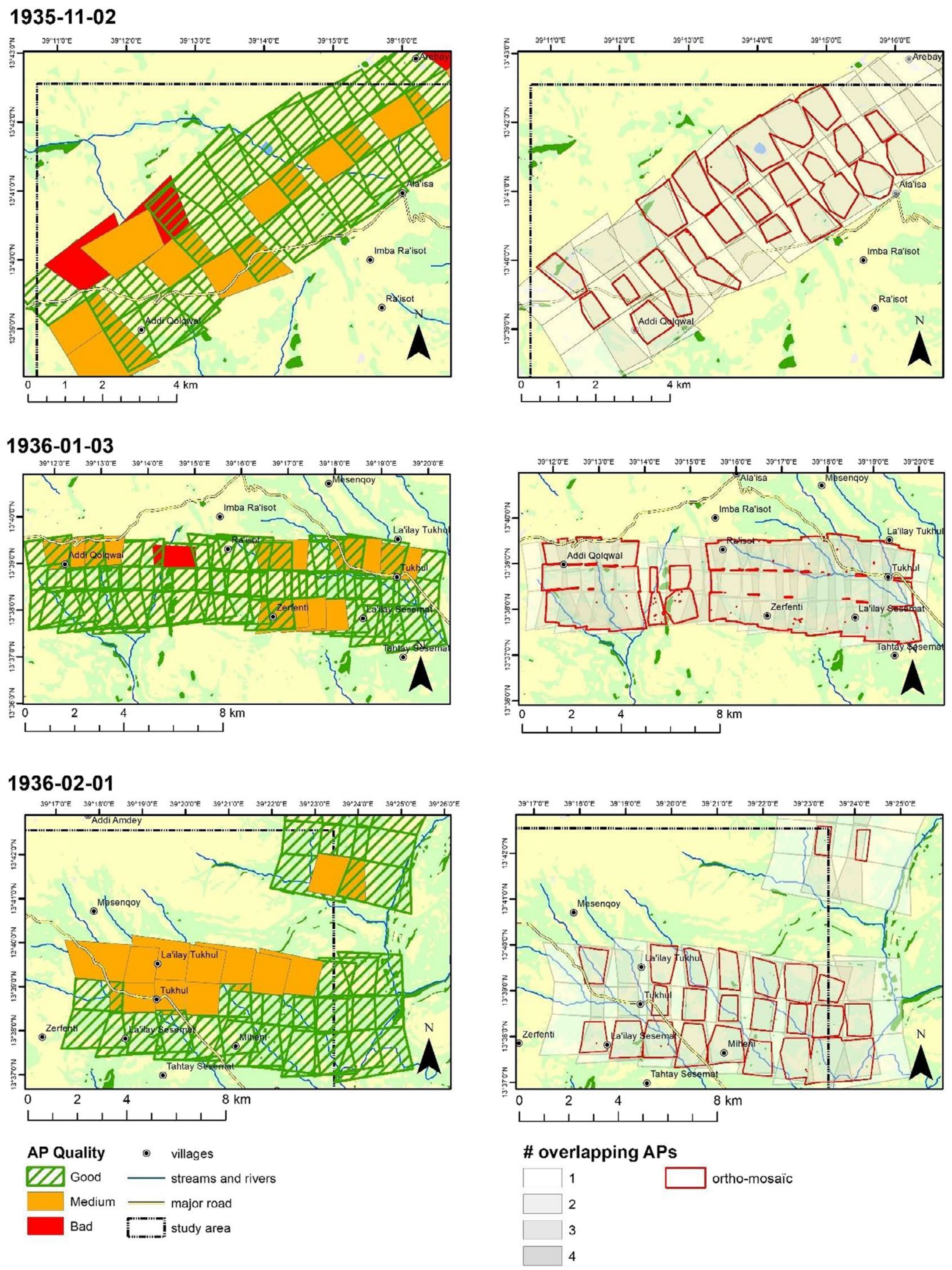

FIGURE 10 Quality of the frames (left) and overlap, resulting in ortho-mosaic coverage (right) for each flight line of Figure 9. 'Bad' quality refers to frames affected for more than 50% by clouds, cloud shadow, poor contrast or damage from storage. Base map: Jacob and Nyssen (2019)

4.4 | Further relocation of photosets

The APs do not at all cover the full country, and the number of photosets is far too small. Besides, within flights some photographs could not be recovered. A major issue is that so far, we failed relocating 5,149 photosets based on merely a few place names in a wider area, particularly those without readily recognizable features. Hence, a semi-automated method to localize and scale these aerial photographs has been tested (Walter & Fritsch, 1999). At first, within an unlocated series of successive photosets, the photographs were aligned to create an ortho-mosaic, and DEM extracted (when sufficient overlap between adjacent photos). The result was used to extract the drainage network of that unknown area (Ariza-Villaverde *et al.*, 2015). Next, similarities were searched with parts of the recent drainage network (extracted from the SRTM30). This comparison was performed by a script to detect matches (Hussnain *et al*., 2016; Mustière & Devogele, 2008). The algorithm was based on Strahler's stream orders of the rivers (Luo *et al*., 2014; Molloy & Stepinski, 2007), the angle difference between the historical an recent segments (Borgefors, 1988) and the scale between both networks (Forceville, 2018).

Though the method was successful on regular imagery taken in 1964, the Italian imagery from the 1930s over Ethiopia could not be relocated through it. Indeed, the algorithm performs best with high stream orders and a long array of consecutive streams, but these were difficult to obtain from the chunks of flight lines available for the studied photosets. Another problem was that incorrect drainage networks were generated because of gaps in the generated DEM and artefacts induced by the borders of the frames (Forceville, 2018).

The best option that remains is manual tracing using Google Earth or similar, possibly as geo-crowdsourcing (Porto De Albuquerque *et al*., 2016; Produit & Ingensand, 2018), in which interested people try to locate photosets from flights in selected approximate coverage areas (Figure 11).

4.5 | Automated aerial photograph interpretation

These historical aerial photographs offer a great opportunity to prolong the timespan over which land cover data, and studies have been undertaken to understand the complexity of land cover changes in a more accurate way (see above). Yet, analogous interpretation of black and white orthophotographs is very time-consuming. The possibilities of such historical aerial imagery for the (semi-) automated extraction

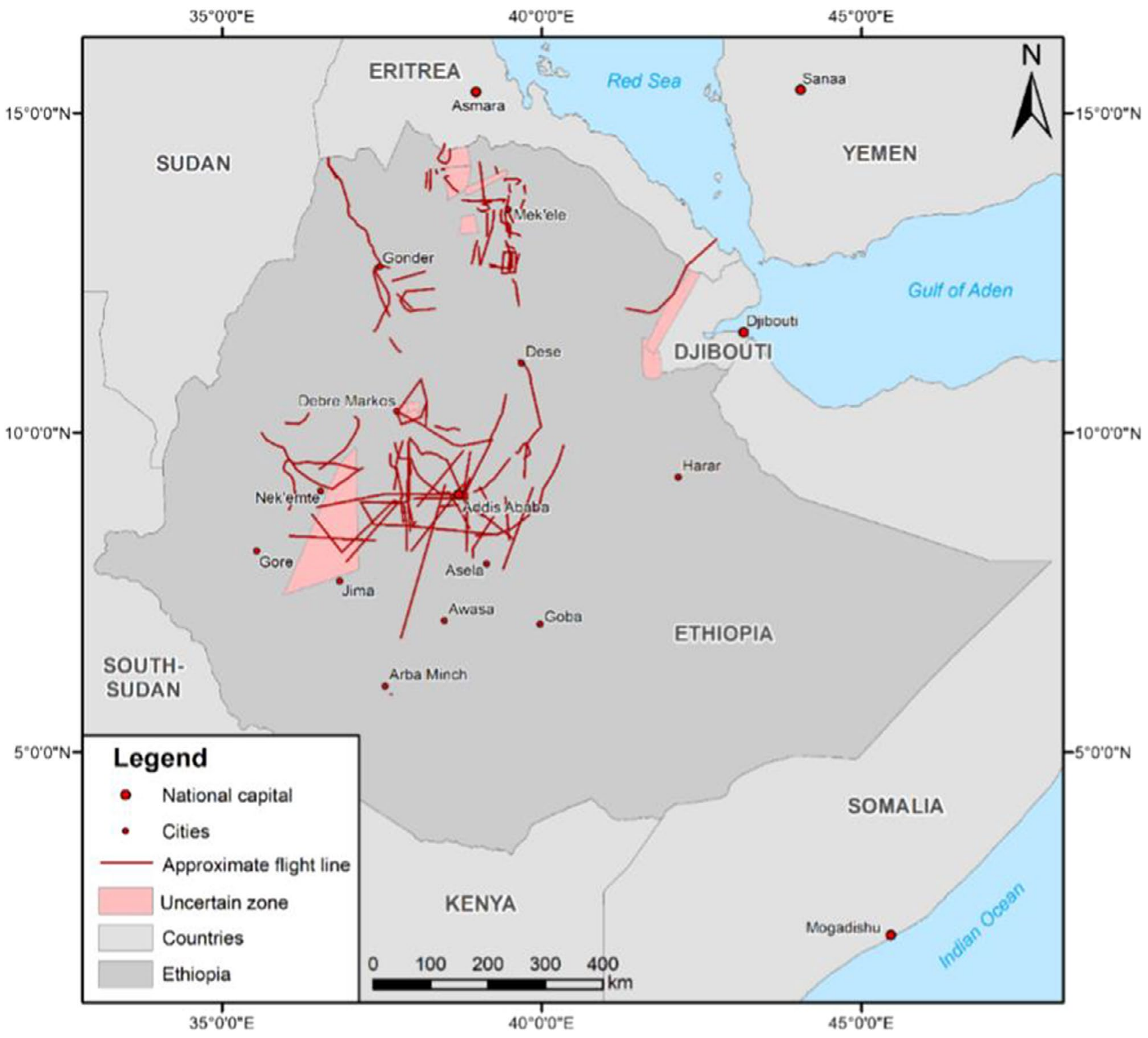

FIGURE 11 Flight lines and approximate areas for which photosets are available, but georeferencing needed

of the land cover classes 'cropland' and 'woody vegetation' were investigated. A subset of the APs was analysed within the study area covering 323 km^2 in the eastern part of the Dogu'a Tembien district in the Tigray region (Figure 1). For the classification of cropland, we applied the combination (Vogels *et al*., 2017) of object-based classification technique and *random forest* machine learning technique (Breiman, 2001; Liaw & Wiener, 2002), of which the classification results achieved a Kappa coefficient (Lillesand *et al*., 2008) between 0.40 and 0.70. From the 22 different object variables that were taken into account during the classification process, textural variables based on the grey-level co-occurrence matrix seemed to play a more important role during the classification process than geometrical variables and the brightness of the objects (Debever, 2019).

In view of the large number of possible objects in areas with woody vegetation, it was preferred to use a pixel-based classification technique for the 'woody vegetation' that was anticipated to appear with a lower brightness (Kadmon & Harari-Kremer, 1999; Sharp & Bowman, 2004). At first, this led to an overestimation of the amount of 'woody vegetation'. Whereas such errors would be corrected through manual editing in case of smaller areas (Frankl *et al*., 2019), for Tembien, the results were optimized by means of a process that integrated the pixel- and object-based approaches (Debever, 2019). These historical APs offer many perspectives for analysing and modelling land cover changes in Ethiopia, but there are challenges related to a sometimes lesser quality of the APs.

ACKNOWLEDGEMENTS

Availing the collection of historical aerial photographs would not have been possible without the strong support by Sultan Mohammed, director of EMA in 2012. The late Gordon Petrie (University of Glasgow) contributed a lot to sharpening our insights in the instrumentation of the 1930s. Further, Koen Hufkens (Harvard University), Neil Munro (Mekelle University) and Maarten Wynants (University of Plymouth) hinted available archives of historical aerial photographs covering parts of Africa. Last but not least, communities in many of the portrayed scenes (Lake Tana basin, Dogu'a Tembien, Kemise graben) are gratefully acknowledged for guiding team members to specific locations of ground control points and other geographical features in the APs.

CONFLICT OF INTERESTS

The authors declare that they have no conflict of interest.

AUTHOR CONTRIBUTIONS

Jan Nyssen traced the collection of aerial photographs, unearthened it, set up the institutional framework, relocated photosets and prepared the manuscript. Martijn Debever evaluated the validity of the data set for change studies, relocated the larger part of photosets and contributed to manuscript writing. Gezahegne Gebremeskel contributed to unearthening the data set and to manuscript writing. Bart De Wit prepared the data set for online availing and contributed to manuscript witing. Kiros Meles Hadgu set up the institutional framework for data set acquisition and contributed to manuscript writing. Steven De Vriese prepared the data set for online availing and contributed to manuscript writing. Jeffrey Verbeurgt prepared the data set for online availing and contributed to manuscript writing. Amaury Frankl evaluated the validity of the data set for preparation of orthophotographs and for change studies, and contributed to manuscript writing. Tulu Besha set up the institutional framework for data set acquisition and critically read the manuscript. Jan Kropáček evaluated the validity of the data set for preparation of orthophotographs and for change studies, and contributed to manuscript writing. Astrid Forceville evaluated the validity of the data set for preparation of orthophotographs and contributed to manuscript writing. Biadgilgn Demissie set up the institutional framework for data set acquisition and contributed to manuscript writing.

DATA AVAILABILITY STATEMENT

The data set of aerial photographs of Ethiopia in the 1930s has been availed to the wider scientific community through the Pangaea website http://doi.org/10.1594/PANGAEA.920077 (Nyssen *et al*., 2020). Selection and downloading of relocated photographs are best done using web interface http://www.ethiopia1935.ugent.be/.

OPEN PRACTICES

This article has earned an Open Data badge for making publicly available the digitally-shareable data necessary to reproduce the reported results. The data is available at https://doi.org/10.1594/PANGAEA.920077 and http://www.ethiopia1935.ugent.be/ Learn more about the Open Practices badges from the Center for OpenScience: https://osf.io/tvyxz/wiki.

ORCID

Jan Nyssen https://orcid.org/0000-0002-2666-3860
Jeffrey Verbeurgt https://orcid.org/0000-0002-9045-6049

REFERENCES

Agisoft (2018) *Agisoft Photoscan User Manual: Professional Edition, Version 1.4*. St. Petersburg, Russia: Agisoft LLC.

Ariza-Villaverde, A., Jiménez-Hornero, F. & De Ravé, E.G. (2015) Influence of DEM resolution on drainage network extraction: a multifractal analysis. *Geomorphology*, 241, 243–254.

Barker, A.J. (1968) *The civilizing mission: the Italo-Ethiopian war of 1935–6*. London, UK: Cassell.

Bellhouse, D. (1981) Area estimation by point-counting techniques. *Biometrics*, 37, 303–312.

Bergaglio, M. (2001) *L'impiego dell'aero nella rilevazione cartografica coloniale durante il conflitto italo-etiopico. Atti del convegno*

Nazionale Cultura cartografica e culture del territorio, 12-13 December 2000, Sassari, Italy, 2001. Genova, Italy: Casa Editrice Brigati Glauco & Co, pp. 573–585.

Borgefors, G. (1988) Hierarchical chamfer matching: A parametric edge matching algorithm. *IEEE Transactions on Pattern Analysis and Machine Intelligence*, 10, 849–865.

Breiman, L. (2001) Random forests. *Machine Learning*, 45, 5–32.

Caswell, T.R. (2012) *Unearthing St. Augustine's Colonial Heritage: An Interactive Digital Collection for the Nation's Oldest City*. Jacksonville, FL: University of North Florida.

Debever, M. (2019) *Semi-automated Land Use/Land Cover Extraction from Historical Aerial Photographs – A Case Study in Dogu'a Tembien (Ethiopia) over the Period 1935–2035*. M.Sc. thesis study, Department of Geography, Ghent University.

DRC Mining (2012) *The Network for the Geological and Mining References in D.R. Congo*. Available at: Tervuren, Belgium: CRGM, CTCPM, CAMI, UNILU and Royal Museum for Central Africa. http://www.drcmining.org/en/index_html (Last accessed on 19/02/2021).

Durham University (2020) *The Sudan Archive at Durham*. Durham, UK: Durham University. Available at: https://www.dur.ac.uk/library/asc/sudan/ (Last accessed on 19/02/2021).

F5 INC (2020) *NGINX*. Seattle, WA: F5 INC. Available at: https://www.nginx.com/ (Last accessed on 19/02/2021).

Forceville, A. (2018) *An algorithm to localise and scale aerial photographs without metadata – the case of Italian imagery over Ethiopia in the 1930s*. M.Sc. thesis study, Department of Geography, Ghent University.

Frankl, A. (2012) *Gully development and its spatio-temporal variability since the late 19th century in the Northern Ethiopian Highlands*. PhD, Ghent University.

Frankl, A., Nyssen, J., Adgo, E., Wassie, A. & Scull, P. (2019) Can woody vegetation in valley bottoms protect from gully erosion? Insights using remote sensing data (1938–2016) from subhumid NW Ethiopia. *Regional Environmental Change*, 19, 2055–2068.

Frankl, A., Seghers, V., Stal, C., De Maeyer, P., Petrie, G. & Nyssen, J. (2015a) Using image-based 3D modelling to produce a 1935 ortho-mosaic of the Ethiopian Highlands. *International Journal of the Digital Earth*, 8(5), 421–430.

Frankl, A., Stal, C., Abraha, A., Nyssen, J., Rieke-Zapp, D., De Wulf, A. et al. (2015b) Detailed recording of gully morphology in 3D through image-based modelling. *Catena*, 127, 92–101.

Gentilli, R. (1992) *Guerra aerea sull'Etiopia 1935–1939*. Florence, Italy: EDAI.

Ghebreyohannes, T., De Meyere, M., Frankl, A., Haile, M. & Nyssen, J. (2018) Regreening of the northern Ethiopian mountains: effects on flooding and on water balance. *Afrika Focus*, 31,129–147.

Ghebreyohannes, T., Frankl, A., Haile, M., Zenebe, A. & Nyssen, J. (2015) Sediment flux dynamics as fingerprints of catchment rehabilitation: the case of western Rift Valley escarpment of northern Ethiopia. *Geomorphology*, 250, 220–235.

Ghent University (2020) *Official public style guide of Ghent University*. Ghent, Belgium: Ghent University. Available at: https://styleguide.ugent.be/?lang=en (Last accessed on 19/02/2021).

Google Search Guides (2020). *Mobile-first Indexing Best Practices*. Available at: Mountain View, CA, USA: Google Inc. https://developers.google.com/search/mobile-sites/mobile-first-indexing. (Last accessed on 19/02/2021)

Guyassa, E., Frankl, A., Lanckriet, S., Demissie, B., Zenebe, G., Zenebe, A. et al. (2018b) Changes in land use/cover mapped over 80 years in the Highlands of Northern Ethiopia. *Journal of Geographical Sciences*, 28, 1538–1563.

Guyassa, E., Frankl, A., Zenebe, A., Poesen, J. & Nyssen, J. (2018a) Gully and soil and water conservation structure densities in semi-arid northern Ethiopia over the last 80 years. *Earth Surface Processes and Landforms*, 43, 1848–1859.

Hearn, G.J. (2019) Slope hazards on the Ethiopian road network. *Quarterly Journal of Engineering Geology and Hydrogeology*, 52, 295–311.

Hishe, S., Bewket, W., Nyssen, J. & Lyimo, J. (2020) Analysing past land use land cover change and CA-Markov-based future modelling in the Middle Suluh Valley, Northern Ethiopia. *Geocarto International*, 35, 225–255.

Hughes, M.L., McDowell, P.F. & Marcus, W.A. (2006) Accuracy assessment of georectified aerial photographs: Implications for measuring lateral channel movement in a GIS. *Geomorphology*, 74, 1–16.

Hussnain, Z., Oude Elberink, S. & Vosselman, G. (2016) Automatic feature detection, description and matching from mobile laser scanning data and aerial imagery. *International Archives of the Photogrammetry, Remote Sensing & Spatial Information Sciences*, 41, 609–616.

IGM (1939) *L'Istituto Geografico Militare in Africa Orientale, 1885–1937*. Roma, Italy: Istituto Geografico Militare.

IWM (2020) *Imperial War Museums Collection*. London, UK: IWM. Available at: www.iwm.ac.uk (Last accessed on 19/02/2021).

Jacob, M. (2015) *Treeline dynamics and forest cover change in afro-alpine Ethiopia, as affected by climate change and anthropo-zoogenic impacts*. PhD thesis, Department of Geography, Ghent University, Ghent, Belgium.

Jacob, M. & Nyssen, J. (2019) Dogu'a Tembien geo-trekking map at 1:50,000. In: Nyssen, J., Jacob, M. & Frankl, A. (Eds.) *Geo-Trekking in Ethiopia's Tropical Mountains, the Dogu'a Tembien District*. Heidelberg, Germany: Springer Nature.

James, M.R., Chandler, J.H., Eltner, A., Fraser, C., Miller, P.E., Mills, J.P. et al. (2019) Guidelines on the use of structure-from-motion photogrammetry in geomorphic research. *Earth Surface Processes and Landforms*, 44, 2081–2084.

James, M.R. & Robson, S. (2012). Straightforward reconstruction of 3D surfaces and topography with a camera: accuracy and geoscience application. *Journal of Geophysical Research: Earth Surface*, 117(F03017), 1–17.

Kadmon, R. & Harari-Kremer, R. (1999) Studying long-term vegetation dynamics using digital processing of historical aerial photographs. *Remote Sensing of Environment*, 68, 164–176.

Kassa, G., Crummey, D., Descheemaeker, K. & Nyssen, J. (2011) Land degradation and resilience in Wollo from the 1930s onwards, as derived from aerial and terrestrial photographs. In: Nyssen, J., Asrat, A., Dramis, F. & Umer, M. (Eds.) *Excursion Guide to the North Ethiopian Highlands. International Association of Geomorphologists, Regional Conference 2011, Addis Ababa*.

Köbben, B. (2014) Een Nationale Atlas in de Nationale GeoData Infrastructuur. *Geo-Info*, 2014-2, 18–21.

Kropáček, J., Vařilová, Z. & Nyssen, J. (2019) Historical aerial and terrestrial photographs for the investigation of mass movement dynamics in the Ethiopian Highlands. *Land Degradation & Development*, 30, 483–493.

Kuns, B. (2010). *Towards an Inventory of Historical Aerial Photos of Kenya, Tanzania and Uganda*. Stockholm: EU FP7 CREATING

Project. https://tanganyikabase.africamuseum.be/aerial_photos_survey.pdf. (last accessed on 19/2/2021)

Lanckriet, S., Derudder, B., Naudts, J., Bauer, H., Deckers, J., Haile, M. et al. (2015) A political ecology perspective of land degradation in the North Ethiopian Highlands. *Land Degradation & Development*, 26, 521–530.

LeafletJS (2020). *Leaflet, An Open-Source JavaScript Library for Mobile-friendly Interactive Maps*. Kyiv, Ukraine: Vladimir Agafonkin. Available at: https://leafletjs.com/ (Last accessed on 19/02/2021).

Liaw, A. & Wiener, M. (2002) Classification and regression by randomForest. *R News*, 2, 18–22.

Lillesand, T.M., Kiefer, R.W. & Chipman, J.W. (2008) *Remote Sensing and Image Interpretation*. New York, NY: John Wiley & Sons Inc.

Long, H., Lage, K. & Cronin, C. (2005) The flight plan of a digital initiatives project, part 2 - Usability testing in the context ofuser-centered design. *OCLC Systems & Services: International digital library perspectives*, 21, 324–345.

Luman, D.E., Stohr, C. & Hunt, L. (1997) Digital reproduction of historical aerial photographic prints for preserving a deteriorating archive. *Photogrammetric Engineering and Remote Sensing*, 63, 1171–1179.

Luo, W., Li, X., Molloy, I., Di, L. & Stepinski, T. (2014) Web service for extracting stream networks from DEM data. *GeoJournal*, 79, 183–193.

Ma, R. (2013) Rational function model in processing historical aerial photographs. *Photogrammetric Engineering & Remote Sensing*, 79, 337–345.

MailJet (2020) *The email solution for fast-moving teams*. Nantes, France: MailJet. Available at: https://www.MailJet.com/ (Last accessed on 19/02/2021).

Massi, E. (1940) Economia dell'Africa Italiana. *Rivista Internazionale di Scienze Sociali, Serie III*, 11, 424–454.

Mathews, L.E. (2005) *Aerial Photography Field Office (AFPO) Historical Imagery Holdings for the United States Department of Agriculture*. Washington, DC: United States Department of Agriculture.

Mcauliffe, C.P., Lage, K. & Mattke, R. (2017) Access to online historical aerial photography collections: Past practice, present state, and future opportunities. *Journal of Map & Geography Libraries*, 13, 198–221.

Merla, G. & Minucci, E. (1938) *Missione geologica nel Tigrai*. Roma, Italy: Reale Accademia d'Italia.

Michel, N. (2018) *Patrimoine: d'anciennes photographies aériennes de l'Afrique menacées de destruction*. Paris, France: Jeune Afrique. Available at: https://www.jeuneafrique.com/677525/culture/patrimoine-danciennes-photographies-aeriennes-de-lafrique-menacees-de-destruction/ (Last accessed on 19/02/2021).

Molloy, I. & Stepinski, T.F. (2007) Automatic mapping of valley networks on Mars. *Computers & Geosciences*, 33, 728–738.

Morgan, J.L., Gergel, S.E. & Coops, N.C. (2010) Aerial photography: a rapidly evolving tool for ecological management. *BioScience*, 60, 47–59.

Mustière, S. & Devogele, T. (2008) Matching networks with different levels of detail. *GeoInformatica*, 12, 435–453.

National Archives (2020) *Records of the U.S. Geological Survey [USGS]*. College Park, MD, USA: National Archives. Available at: https://www.archives.gov/research/guide-fed-records/groups/057.html. (Last accessed on 19/02/2021).

NCAP (2020) *National Collection of Aerial Photography*. Edinburgh, UK: NCAP. Available at: https://ncap.org.uk (Last accessed on 19/02/2021).

NGI (2020) *CDNGI Geospatial Portal*. Cape Town, South Africa: Department of Rural Development and Land Reform, National Geospatial Information. Available at: http://www.cdngiportal.co.za/cdngiportal/ (Last accessed on 19/02/2021).

Nyssen, J., Debever, M., Gebremeskel, G., De Wit, B., Hadgu, K.M., De Vriese, S. et al. (2020) *Aerial photographs of Ethiopia 1935–1941*. Data Publisher for Earth & Environmental Science. Bremen, Germany: PANGAEA. https://doi.pangaea.de/10.1594/PANGAEA.920077.

Nyssen, J. & Denaeyer, A. (2019) Unequal access to land or equity: impacts on land degradation around Lake Ashenge. In: Nyssen, J., Demissie, B. and Ghebreyohannes, T. (Eds.) *Land, Water, People and Landscapes in North Ethiopia's Grabens*. Mekelle (Tigray, Ethiopia) and Ghent (Belgium): VLIR-UOS, Mekelle University, Ghent University, KU Leuven, pp. (68–72).

Nyssen, J., Petrie, G., Mohamed, S., Gebremeskel, G., Seghers, V., Debever, M. et al. (2016) Recovery of the historical aerial photographs of Ethiopia in the 1930s. *Journal of Cultural Heritage*, 17, 170–178.

Nyssen, J., Petrie, G., Munro, R.N., Jacob, M., Smidt, W., Haile, M. et al. (2019) Historical maps, terrestrial and aerial photographs. In: Nyssen, J., Jacob, M. and Frankl, A. (Eds.) *Geo-trekking in Ethiopia's Tropical Mountains*. Cham, Switzerland: Springer, pp. (461–476).

OpenJS Foundation (2020) *nodeJS*. San Francisco, CA: OpenJS Foundation. Available at: https://nodejs.org/en/ (Last accessed on 19/02/2021).

Persia, M., Barca, E., Greco, R., Marzulli, M. & Tartarino, P. (2020) Archival aerial images georeferencing: a geostatistically-based approach for improving orthophoto accuracy with minimal number of ground control points. *Remote Sensing*, 12, 2232.

Peterson, E.B. (2017) *Aerial Photography from 1960 Orthorectified and a Digital Surface Model Derived with Structure-from-Motion Photogrammetry. Downloadable Data Package*. Weaverville, CA: Trinity River Restoration Program (TRRP).

Pinto, A.T., Gonçalves, J.A., Beja, P. & Pradinho Honrado, J. (2019) From archived historical aerial imagery to informative orthophotos: a framework for retrieving the past in long-term socioecological research. *Remote Sensing*, 11, 1388.

Podestà, G.-L. (2013) Building the empire. Public works in Italian East Africa (1936–1941). *Entreprises et Histoire*, 70, 37–53.

Porto De Albuquerque, J., Herfort, B. & Eckle, M. (2016) The tasks of the crowd: A typology of tasks in geographic information crowdsourcing and a case study in humanitarian mapping. *Remote Sensing*, 8, 859.

Produit, T. & Ingensand, J. (2018) 3D georeferencing of historical photos by volunteers. In: Mansourian, A., Pilesjö, P., Harrie, L. and Van Lammeren, R. (Eds.) *Geospatial Technologies for All*. Cham, Switzerland: Springer, pp. (113–128).

Pullan, R. (1976) The history and use of aerial photography in Zambia. *Zambia Geographical Journal*, 31, 33–52.

Sarabadani Tafreshi, A.E., Marbach, K. & Norrie, M.C. (2017) Proximity-based adaptation of web content on public displays. In: Cabot, J., De Virgilio, R. & Torlone, R. (Eds.) *Web Engineering. ICWE 2017. Lecture Notes in Computer Science*. Cham, Switzerland: Springer International Publishing.

Schade, A. (2014) *Responsive Web Design (RWD) and User Experience*. Fremont, CA, USA: Niels Norman Group. Available at: https://www.nngroup.com/articles/responsive-web-design-definition/ (Last accessed on 19/02/2021).

Schermerhorn, W. (1970) In memoriam. Dr. H.c. Ing. Ermenegildo Santoni (1896–1970). *Photogrammetria*, 26, 37–39.

Scull, P., Cardelús, C.L., Klepeis, P., Woods, C.L., Frankl, A. & Nyssen, J. (2017) The resilience of Ethiopian church forests: interpreting aerial photographs, 1938–2015. *Land Degradation & Development*, 28, 450–458.

Seitz, S., Curless, B., Diebel, J., Scharstein, D. & Szeliski, R. (2006) *A comparison and evaluation of multi-view stereo reconstruction algorithms*. IEEE Computer Society Conference on Computer Vision and Pattern Recognition. New York, NY, USA.

Sevara, C., Verhoeven, G., Doneus, M. & Draganits, E. (2018) Surfaces from the visual past: Recovering high-resolution terrain data from historic aerial imagery for multitemporal landscape analysis. *Journal of archaeological method and theory*, 25, 611–642.

Sharp, B.R. & Bowman, D.M. (2004) Patterns of long-term woody vegetation change in a sandstone-plateau savanna woodland, Northern Territory, Australia. *Journal of Tropical Ecology*, 20, 259–270.

Smith, T.J. III, Tiling-Range, G., Jones, J., Nelson, P., Foster, A., Balentine, K., & (2010) The use of historical charts and photographs in ecosystem restoration: examples from the Everglades Historical Air Photo Project. In: David C. Cowley Robin A. Standring & Matthew J. Abicht *Landscapes through the Lens: Aerial Photographs and the Historic Environment*. Oxford, UK: Oxbow Books, pp. (179–191), vol 2.

Taylor, M.A. (2019) *Using GIS to Identify Potential Dynamic Marine Protected Areas: A Case Study using Shortfin Mako Shark Tagging Data in New Zealand*. Los Angeles, CA: University of Southern California.

Traversi, C. (1964) *L'Italia in Africa. Storia della cartografia coloniale Italiana*. Roma, Italy: Poligrafico dello Stato.

Vogels, M.F., De Jong, S.M., Sterk, G. & Addink, E.A. (2017) Agricultural cropland mapping using black-and-white aerial photography, object-based image analysis and random forests. *International Journal of Applied Earth Observation and Geoinformation*, 54, 114–123.

Walter, V. & Fritsch, D. (1999) Matching spatial data sets: a statistical approach. *International Journal of geographical information science*, 13, 445–473.

Whitlow, R. (1988) Aerial photography in Zimbabwe, 1935–1986. *Zambezia*, XV, 137–165.

Wilson, A.T., Miles, H.C., Labrosse, F., Tiddeman, B. & Roberts, J.C. (2016) Historical records, archives and photogrammetry. *The Historic Environment: Policy & Practice*, 7, 25–42.

WOSSAC (2020). *World Soil Survey Archive and Catalogue*. Cranfield, UK: Centre for Environmental & Agricultural Informatics, Cranfield University. Available at: www.wossac.com (Last accessed on 19/02/2021).

Zeimetz, K.A., Dillon, E., Hardy, E.E. & Otte, R.C. (1976) Using area point samples and airphotos to estimate land use change. *Agricultural Economics Research*, 28, 65–74.

How to cite this article: Nyssen J, Debever M, Gebremeskel G, et al. Online digital archive of aerial photographs (1935–1941) of Ethiopia. *Geosci Data J*. 2021;00:1–34. https://doi.org/10.1002/gdj3.115

APPENDIX A

Python script for filename consistency

```
# -*- coding: utf-8 -*-
"""
Created on Mon May 11 13:13:24 2020

@author: Jeffrey Verbeurgt

This script is used to check all filenames of the .TIF-files.
The .TIF-files are located in the original directories, which are
named after
date of acquisition. The .TIF-files are either aerial pictures or
the label
describing details of an aerial picture. The general structure of
the filenames
is:
    [filename]-[photonumber]-[startnumber serie]-[endnumber
serie].TIF
    OR
    [filename]-[photonumber]-[startnumber serie]-[endnumber
serie]-label.TIF

The script generates three logfiles:
    1. Summary containing the number of accepted and rejected
filenames
    2. File containing all accepted filenames and their location
    3. File containing all rejetped filenames and their location

Based on the logfiles, the filenames can be manually adapted to
conform to the
filenaming structure.
"""
###################################################################
#############
# import modules
###################################################################
#############
import os #to loop over files in directories
import re #to use regular expressions on the filenames
import datetime #to timestamp the log-files


###################################################################
#############
# user defined settings for location of input and output
###################################################################
#############
#define the directory containing files in subdirectories
directory = "."


###################################################################
#############
# create the logfiles
###################################################################
#############
```

```
#Use timestamp to separate logfiles from different runs
timestamp = datetime.datetime.now().strftime("%Y %m %d %H_%M_%S")

#create log files: summary, correct filenames, wrong filenames
#create a string which will contain full log for each file
log_summary = "log filename summary for run
{}\n".format(timestamp)
log_summary_filename = str("01_" +
                           log_summary.rstrip('\n').replace("
","_") +
                           ".log") #name of logfile

log_wrong = "log filename wrong filenames for run
{}\n".format(timestamp)
log_wrong_filename = str("01_" +
                         log_wrong.rstrip('\n').replace(" ","_") +
                         ".log") #name of logfile

log_correct = "log filename correct filenames for run
{}\n".format(timestamp)
log_correct_filename = str("01_" +
                           log_correct.rstrip('\n').replace("
","_") +
                           ".log") #name of logfile

#Some counters to use in the logfiles
counter_wrong_filenames = 0
counter_correct_filenames = 0
counter_total_filenames = 0


##################################################################
#############
# Actual filenaming analysis
##################################################################
#############
#get a list of all sub-directories in parent directory
my_dirs = [d for d in os.listdir(directory) if
os.path.isdir(os.path.join(directory, d))]

#define patterns for the regular expressions
pattern_label = '^.*-[0-9]*-[0-9]*-[0-9]*-label\.tif$' #pattern
for label files
pattern_aerial = '^.*-[0-9]*-[0-9]*-[0-9]*\.tif$' #pattern for
aerial files

#loop over all files in all directories
for directory in my_dirs: #loop over each dir
    log_wrong += ("DIR: " + str(directory) + "\n") #append current
dir to log
    log_correct += ("DIR: " + str(directory) + "\n") #append
current dir to log
    for filename in os.listdir(directory): #loop over each file in
dir
        counter_total_filenames += 1 #add 1 to count of total
files
        #Get boolean value for match with regex pattern
        result_label = re.match(pattern_label, filename.lower())
        result_aerial = re.match(pattern_aerial, filename.lower())
        if result_label and not result_aerial: #if match with
label regex
            counter_correct_filenames += 1 #add 1 to counter of
accepted files
            log_correct += "{}\n".format(filename) #write filename
to log

        elif result_aerial and  not result_label: #if match with
aerial regex
            counter_correct_filenames += 1 #add 1 to counter of
accepted files
            log_correct += "{}\n".format(filename) #write filename
to log

        else: #if filename not matches
            counter_wrong_filenames += 1 #add 1 to counter of
rejected files
            log_wrong += "{}\n".format(filename) #write filename
to log

    #do this at end of looping over all files of a dir
    #this is purely for esthetical reasons in the logfiles
    log_wrong += (("#"*80)+"\n")
    log_correct += (("#"*80)+"\n")


###################################################################
#############
# Write results to logfiles
###################################################################
#############
with open(log_summary_filename, "w") as log_summary_file:
    log_summary_file.write(log_summary)
    log_summary_file.write("Number rejected
files:\t{}\n".format(counter_wrong_filenames))
    log_summary_file.write("Number accepted
files:\t{}\n".format(counter_correct_filenames))
    log_summary_file.write("Number total
files:\t{}\n".format(counter_total_filenames))

with open(log_correct_filename, "w") as log_correct_file:
    log_correct_file.write(log_correct)

with open(log_wrong_filename, "w") as log_wrong_file:
    log_wrong_file.write(log_wrong)
```

APPENDIX B

Python script for consolidation of filenames and conversion to .JPG

```
# -*- coding: utf-8 -*-
"""
Created on Mon May 11 20:24:34 2020

@author: Jeffrey Verbeurgt

This is the second script to be used in the process of the file
renaming.

Make sure all filenames are conform the following structure:
    [filename]-[photonumber]-[startnumber serie]-[endnumber
serie].TIF
    OR
    [filename]-[photonumber]-[startnumber serie]-[endnumber
serie]-label.TIF

The script renames and converts the files, output is stored in one
folder.
Renaming according to following structure:
    [DIRNAME]-[photonumber]-[filename]-[photonumber]-[startnumber
serie]-[endnumber serie].TIF
    OR
    [DIRNAME]-[photonumber]-[filename]-[photonumber]-[startnumber
serie]-[endnumber serie]-label.TIF

The original .TIF-files are converted to JPEG-files. Settings are
used which
reduce filesize with 90% without giving up on much quality.
"""
###################################################################
#############
# import modules
###################################################################
#############
import os #to loop over files in directories
import re #to use regular expressions on the filenames
import datetime #to timestamp the log-files
from PIL import Image #to convert TIF to JPEG


###################################################################
#############
# user defined settings for location of input and output
###################################################################
#############
#define the directory containing files in subdirectories
mypath = "."
outpath_accepted = "accepted_files_output" #for TIF=>JPEG with
correct filename
outpath_rejected = "rejected_files_output" #for TIF=>JPEG with
wrong filename


###################################################################
#############
# create the logfiles
###################################################################
#############
#Use timestamp to separate logfiles from different runs

timestamp = datetime.datetime.now().strftime("%Y %m %d %H_%M_%S")

#create log files: summary, succesful filenames, failed filenames
#create a string which will contain full log for each file
```

```
log_summary = "log rename and convert summary for run
{}\n".format(timestamp)
log_summary_filename = mypath + "/" + str("02_" +

log_summary.rstrip('\n').replace(" ","_") +
                                          ".log")

log_failed = "log failed rename and convert for run
{}\n".format(timestamp)
log_failed_filename = mypath + "/" + str("02_" +

log_failed.rstrip('\n').replace(" ","_") +
                                         ".log")

log_succes = "log succesful rename and convert for run
{}\n".format(timestamp)
log_succes_filename = mypath + "/" + str("02_" +

log_succes.rstrip('\n').replace(" ","_") +
                                         ".log")

#Some counters to use in the logfiles
counter_failed_files = 0
counter_succes_files = 0
counter_total_files = 0


##################################################################
#############
# Perform actual analysis to rename and convert each file
##################################################################
#############
#define patterns for the regular expressions
pattern_label = '^.*-[0-9]*-[0-9]*-[0-9]*-label$' #pattern for
label files
pattern_aerial = '^.*-[0-9]*-[0-9]*-[0-9]*$' #pattern for aerial
files

for root, dirs, files in os.walk(mypath, topdown=False):
    for name in files:
        g2g = 0 #good2go==1 means correct filename, 0 means
something wrong
        #First test whether the file under analysis is a TIF
        if os.path.splitext(os.path.join(root, name))[1].lower()
== ".tif":
            counter_total_files += 1 #if tif, add 1 to total # of
files
            filename = os.path.splitext(name)[0] #get rid of
extension

            #Get boolean value for match with regex pattern
            result_label = re.match(pattern_label, filename)
#regex matching
            result_aerial = re.match(pattern_aerial, filename)
#regex matching

            #Depending on filename, a different method is used to
construct the
            #output filename
            if result_label and not result_aerial: #if match with
label regex
```

```
                location, number, series1, series2, label =
filename.rsplit('-',4)
                new_filename = str(os.path.basename(root)) + "-" +
number + "-" + filename
                g2g = 1 #File is according to filenaming structure
            elif result_aerial and  not result_label: #if match
with aerial regex
                location, number, series1, series2 =
filename.rsplit('-',3)
                new_filename = str(os.path.basename(root)) + "-" +
number + "-" + filename
                g2g = 1 #File is according to filenaming structure
            else:
                new_filename = root + "-" + filename
                log_failed += ("Something wrong with filename
{}\n".format(os.path.join(root, name)))

            #Print to stdout to inform researcher on progress
            print(filename + "\n" + new_filename + "\n\n")

            #test if already converted in previous run + if
correct filename
            if os.path.isfile(os.path.join(mypath,
outpath_accepted, new_filename) + ".jpg") and g2g == 1:
                counter_succes_files += 1

            # If a jpeg is *NOT* present + correct filename:
create JPEG
            elif not os.path.isfile(os.path.join(mypath,
outpath_accepted, new_filename) + ".jpg") and g2g == 1:
                outfile = os.path.join(mypath, outpath_accepted,
new_filename) + ".jpg"
                try:
                    im = Image.open(os.path.join(root, name))
                    im.thumbnail(im.size)
                    #see:
https://jdhao.github.io/2019/07/20/pil_jpeg_image_quality/
                    im.save(outfile, "JPEG", quality=95,
subsampling=0)
                    log_succes += ("succesful jpeg for {} to
{}\n".format(name, new_filename))
                    log_succes += ("Old file:
{}\n".format(os.path.join(root, name)))
                    log_succes += ("New file:
{}\n\n".format(outfile))
                    counter_succes_files += 1
                except:
                    log_failed += ("exception: jpeg for {} to
{}\n".format(name, new_filename))
                    log_succes = log_succes.rsplit("\n",4)[0]
#Remove lines written to succes log
                    counter_succes_files -= 1
                    counter_failed_files += 1

            #test if already converted in previous run + wrong
filenameformat
            elif os.path.isfile(os.path.join(mypath,
outpath_rejected, new_filename) + ".jpg") and g2g == 0:
```

```
                log_failed += ("Already converted file
{}\n".format(os.path.join(root, name)))
                counter_succes_files += 1

            # If a jpeg is *NOT* present + wrong filenameformat:
create JPEG
            else:
                outfile = os.path.join(mypath, outpath_rejected,
new_filename) + ".jpg"
                try:
                    im = Image.open(os.path.join(root, name))
                    im.thumbnail(im.size)
                    #see:
https://jdhao.github.io/2019/07/20/pil_jpeg_image_quality/
                    im.save(outfile, "JPEG", quality=95,
subsampling=0)
                    log_succes += ("succesful jpeg for {} to
{}\n".format(name, new_filename))
                    log_succes += ("Old file:
{}\n".format(os.path.join(root, name)))
                    log_succes += ("New file:
{}\n\n".format(outfile))
                    counter_succes_files += 1
                except:
                    log_failed += ("exception: jpeg for {} to
{}\n".format(name, new_filename))
                    log_succes = log_succes.rsplit("\n",4)[0]
#Remove lines written to succes log
                    counter_succes_files -= 1
                    counter_failed_files += 1


##################################################################
#############
# Write results to logfiles
##################################################################
#############
with open(log_summary_filename, "w") as log_summary_file:
    log_summary_file.write(log_summary)
    log_summary_file.write("Number
succes:\t{}\n".format(counter_failed_files))
    log_summary_file.write("Number
failure:\t{}\n".format(counter_succes_files))
    log_summary_file.write("Number
total:\t{}\n".format(counter_total_files))

with open(log_succes_filename, "w") as log_succes_file:
    log_succes_file.write(log_succes)

with open(log_failed_filename, "w") as log_failed_file:
    log_failed_file.write(log_failed)
```

APPENDIX C

Python script for reading all .JPG in a .CSV file

```
# -*- coding: utf-8 -*-
"""
Created on Tue May 12 21:21:22 2020

@author: Jeffrey Verbeurgt

This script reads in a file containing in each row a key-value, X
and Y
The key-value has following structure:
    [YEAR]-[MONTH]-[DAY], [photonumber]

In the next step, the script reads in all JPEG-files in a
directory, extracts
the key-value from the filename and looks up whether the key exist
in the
input. When a match is found, the filename is combined with the
key and the
coordinates in an output file. If no match is found, the filenames
and
constructed key are written to a second file.
"""
##################################################################
#############
# import modules
##################################################################
#############
import os
import pandas as pd


##################################################################
#############
# user defined settings for location of input and output
##################################################################
#############
#define the working dir (dir containing the folder with all JPEG)
workdir = "Z:\shares\we12fg\AERIAL_ETHIOPIA"
os.chdir(workdir)

#give the directory with all converted JPEG
mypath = ".\\accepted_files_output"

#give the filename of the input CSV containing key and coordinates
input_filename = "punten_csv met filename 20200528.csv"

#give output filename of matching records
filename_matching = 'located_pictures.txt'

#give output filename of non-matching records
filename_nonmatching = 'nonlocated_pictures.txt'


##################################################################
#############
# Read in input CSV
##################################################################
#############
df_known = pd.read_csv(input_filename) #Read in CSV
df_known = df_known.dropna(axis=0, how='all') #drop all rows with
only nan-values
```

```
#make a dictionary of the known elements, this speeds up the
comparison later on
#Key is date + fotonumber, value is a list with X, Y, and
filenames
dict_known = {}
for index, row in df_known.iterrows():
    dict_known[row[2]] = [row[0], row[1]]

#make a dictionary which we will fill with the unknown elements
dict_unknown = {}


##################################################################
#############
# Loop over all JPEG in the directory as defined above
##################################################################
#############
for filename in os.listdir(mypath):
    if filename.endswith(".jpg"):
        #Extract year, month, day
        datum = filename[0:4] + '-' + filename[4:6] + '-' +
filename[6:8]
        #Construct the key from the filename
        if "bis" in filename:
            key_bis = datum + ", " + filename[12:].split("-")[0] +
"bis" #add date and foto number together
        key = datum + ", " + filename[9:].split("-")[0] #add date
and foto number together

        if key in dict_known: #Check whether constructed key
exists in actual key
            if "bis" in filename:
                dict_known[key_bis].append(filename) #if match,
add filename to row
            else:
                dict_known[key].append(filename) #if match, add
filename to row

        elif key in dict_unknown: #if match with key in unknown,
add filename
            if "bis" in filename:
                dict_unknown[key_bis].append(filename)
            else:
                dict_unknown[key].append(filename)
        else: #if no match, create new key in unknown dict
            if "bis" in filename:
                dict_unknown[key_bis] = [filename]
            else:
                dict_unknown[key] = [filename]
    else: #if not a jpg, skip this file
        continue


##################################################################
#############
# Write dictionaries to txt file
##################################################################
#############
```

```
with open(filename_matching,'w') as file1:
    #First write header
    file1.write("X;Y;key;pictures;labels;nr pictures;nr labels\n")
    for key in dict_known:
        #define an empty line in output string
        line = ""
        #add to output string the X, Y and key (semicolon-
separated)
        line += str(dict_known[key][0]) + ";" +
str(dict_known[key][1]) + ";" + str(key) + ";"
        #Since there are picture-files and label-files, we need to
check each
        #file to which group it belongs
        pictures = [] #list for picture filenames
        labels = [] #list for label filenames
        for element in dict_known[key][2:]:
            if "label" in element.lower():
                labels.append(element)
            else:
                pictures.append(element)
        #add list of picture filenames-semicolon-label filename
        line += str(pictures) + ";" + str(labels) + ";"
        line += str(len(pictures)) + ";" + str(len(labels)) + "\n"
        file1.write(line)


with open(filename_nonmatching,'w') as file2:
    #First write header
    file2.write("key;pictures;labels;nr pictures;nr labels\n")
    for key in dict_unknown:
        #define an empty line in output string
        line = ""
        #add to output string the X, Y and key (semicolon-
separated)
        line += str(key) + ";"
        #Since there are picture-files and label-files, we need to
check each
        #file to which group it belongs
        pictures = [] #list for picture filenames
        labels = [] #list for label filenames
        for element in dict_unknown[key]:
            if "label" in element.lower():
                labels.append(element)
            else:
                pictures.append(element)
        #add list of picture filenames-semicolon-label filename
        line += str(pictures) + ";" + str(labels) + ";"
        line += str(len(pictures)) + ";" + str(len(labels)) + "\n"
        file2.write(line)
```

APPENDIX D

Script for interactive map

```
// References to DOM elements
var btnOrder = document.getElementById("btn-order");
var itemsInList = document.getElementById("items-in-list");
var requestedItems = document.getElementById("requested-items");
var txtRequests = document.getElementById("requests");
var txtRequestsFeedback = document.getElementById("requests-
feedback");
var mapRef = document.getElementById("osm-map");
var selectionsList = document.getElementById("selections-list");
var orderForm = document.getElementById("order-form");
var overlay = document.getElementById("overlay-wrap");
var txtName = document.querySelector("input[name=name]");
var txtWork = document.querySelector("input[name=work]");
var txtResearch = document.querySelector("input[name=research]");
var txtContributors =
document.querySelector("input[name=contributors]");
var txtEmail = document.querySelector("input[name=email]");
var agree1 = document.querySelector("input[name=agree_1]");
var agree2 = document.querySelector("input[name=agree_2]");
var btnSubmitOrder = document.getElementById("btn-submit-order");
var btnCancelOrder = document.getElementById("btn-cancel-order");

// Array that will hold users selection
var arrOrders = [];

// Supported tile layers
topoLayer =
L.tileLayer("https://a.tile.openstreetmap.org/{z}/{x}/{y}.png", {
      maxZoom: 17
})
var cycleLayer = L.tileLayer("https://a.tile-
cyclosm.openstreetmap.fr/cyclosm/{z}/{x}/{y}.png", {
      maxZoom: 17
})
var aerialLayer =
L.tileLayer("https://server.arcgisonline.com/ArcGIS/rest/services/
World_Imagery/MapServer/tile/{z}/{y}/{x}", {
      maxZoom: 17
})

// For use in map legend
var baseLayers = {
      "OpenStreetMap": topoLayer,
      "Satellite": aerialLayer,
      "OSM topography": cycleLayer
};

// Add map (view settings replaced by map.fitBounds (from geojson
data))
var map = L.map('osm-map', {
      center: [14.096621
06589108, 39.115447998046875],
      zoom: 10,
      layers: [topoLayer]
});
L.control.layers(baseLayers, null,{collapsed:false}).addTo(map);

// Array for all markers
var arrMarkers = []

// Add layer with all markers
var markersLayer = L.geoJSON([data], {
      onEachFeature: onEachFeature,
      pointToLayer: function (feature, latlng) {
            return arrMarkers[feature.properties.Name] =
L.circle(latlng, {
                  radius: 1000,
                  fillColor: "#e9f0fa",
                  color: "#1E64C8",
                  weight: 1,
                  opacity: 1,
                  fillOpacity: 0.9
            });
      }
}).addTo(map);

// Add click event to marker; show popup with photo name
function onEachFeature(feature, layer) {
    layer.on('click', function (e) {
        onMarkerClick(feature.properties.Name);
    });
      //layer.bindPopup(feature.properties.Name.replace('.TIF','')
, {closeButton: false});
      //layer.on('mouseover', function() { layer.openPopup(); });
      //layer.on('mouseout', function() { layer.closePopup(); });
}

// Zoom to all markers
map.fitBounds(markersLayer.getBounds());

// Event handler for marker clicks
function onMarkerClick(markerName) {
      if (arrOrders.indexOf(markerName) === -1) {
            // Add to order list
            if (arrOrders.length < 20) {
                  // Change color to indicate selection
                  setMarkerColor(markerName, '#1E64C8');
                  arrOrders.push(markerName);
            } else {
                  alert("Maximum of 20 photographs reached.")
            }
      } else {
            // Change color back to default
            setMarkerColor(markerName, '#e9f0fa')
            // Remove from order list
            arrOrders = arrOrders.filter(function(item) {
                  return item !== markerName
            })
      }
      updateListCount();
      processSelectionsList();
}

function processSelectionsList() {
      var selectionsHtml = '';
      arrOrders.forEach(function(item) {
            selectionsHtml += '<li>' + item.replace('.jpg','') +
'</li>';
      })
      if (arrOrders.length === 0)  selectionsHtml += '<li>-</li>';
      selectionsList.innerHTML = selectionsHtml;
}
```

```
// Will update the list count in page and enable order button when
selections exist
function updateListCount() {
      itemsInList.innerHTML = arrOrders.length === 1 ? '1 item ' :
arrOrders.length + ' items ';
      requestedItems.innerHTML = arrOrders.length;
      btnOrder.disabled = arrOrders.length === 0 ? true : false;
}

// Change a marker's color
function setMarkerColor(markerName, color){
      arrMarkers[markerName].setStyle({fillColor : color})
}

// Event handler for order button clicks
btnOrder.onclick = function() {
      var requestsStr = '';
      var requestsFeedbackStr = '';
     arrOrders.forEach(function (item) {
            var lng =  data.features.filter(e => e.properties.Name
=== item)[0].properties.X;
            var lat =  data.features.filter(e => e.properties.Name
=== item)[0].properties.Y;
            var point = new GeoPoint(lng, lat)
            requestsStr += item.replace('.jpg','') + '<br>';
      requestsStr += 'Photo: http://we12s018.ugent.be/download/' +
window.btoa(item) + '<br>';
            requestsStr += 'Label:
http://we12s018.ugent.be/download/' +
window.btoa(item.replace('.jpg','-label.jpg')) + '<br>';
            requestsStr += 'Location of principal point: lat ' +
point.getLatDeg() + ', long ' + point.getLonDeg() + '<br><br>';
            requestsFeedbackStr += item.replace('.jpg','') +
'<br>';
     })
     txtRequests.value = requestsStr;
     requestsFeedback.value = requestsFeedbackStr;
      overlay.style.display = "block";
      return false;
}

// Event handler for order button clicks
// Checks user input and submits form
btnSubmitOrder.onclick = function() {
      if (txtName.value.length === 0 ||
                  txtWork.value.length === 0 ||
                  txtResearch.value.length === 0 ||
                  txtContributors.value.length === 0 ||
                  txtEmail.value.length === 0 ) {
            alert("Please fill out all form fields.");
            return false;
      }
      if (!isEmail(txtEmail.value)) {
            alert("Please enter a valid email address.");
            return false;
      }
      if (!agree1.checked || !agree2.checked) {
            alert("Please confirm you agree with our terms.");
            return false;
      }
      if (txtEmail.value.toUpperCase().indexOf('GMAIL') > -1 ||
            txtEmail.value.toUpperCase().indexOf('YAHOO') > -1 ||
            txtEmail.value.toUpperCase().indexOf('HOTMAIL') > -1
||
            txtEmail.value.toUpperCase().indexOf('AOL') > -1 ||
            txtEmail.value.toUpperCase().indexOf('OUTLOOK') > -1
||
            txtEmail.value.toUpperCase().indexOf('ZOHO') > -1 ||
            txtEmail.value.toUpperCase().indexOf('YANDEX') > -1 ||
            txtEmail.value.toUpperCase().indexOf('ICLOUD') > -1 ||
            txtEmail.value.toUpperCase().indexOf('GMX') > -1 ||
            txtEmail.value.toUpperCase().indexOf('PROTONMAIL') > -
1 ||
            txtEmail.value.toUpperCase().indexOf('TUTANOTA') > -1)
{
            alert("Please use an institutional email address.");
            return false;
      }
      orderForm.submit();
}

btnCancelOrder.onclick = function() {
      overlay.style.display = "none";
}


function isEmail(email) {
      var regex = /^([a-zA-Z0-9_.+-])+\@(([a-zA-Z0-9-])+\.)+([a-
zA-Z0-9]{2,4})+$/;
      return regex.test(email);
}


// Conversion GPS to coordinates
GeoPoint=function(t,e){switch(typeof
t){case"number":this.lonDeg=this.dec2deg(t,this.MAX_LON),this.lonD
ec=t;break;case"string":this.decode(t)&&(this.lonDeg=t),this.lonDe
c=this.deg2dec(t,this.MAX_LON)}switch(typeof
e){case"number":this.latDeg=this.dec2deg(e,this.MAX_LAT),this.latD
ec=e;break;case"string":this.decode(e)&&(this.latDeg=e),this.latDe
c=this.deg2dec(e,this.MAX_LAT)}},GeoPoint.prototype={CHAR_DEG:"°",
CHAR_MIN:"'",CHAR_SEC:'"',CHAR_SEP:"
",MAX_LON:180,MAX_LAT:90,lonDec:NaN,latDec:NaN,lonDeg:NaN,latDeg:N
aN,dec2deg:function(t,e){var i=t<0?-
1:1,s=Math.abs(Math.round(1e6*t));if(s>1e6*e)return NaN;var
a=s%1e6/1e6,n=Math.floor(s/1e6)*i,o=Math.floor(60*a),h=3600*(a-
o/60),r="";return
r+=n,r+=this.CHAR_DEG,r+=this.CHAR_SEP,r+=o,r+=this.CHAR_MIN,r+=th
is.CHAR_SEP,r+=h.toFixed(2),r+=this.CHAR_SEC},deg2dec:function(t){
var e=this.decode(t);if(!e)return NaN;var
i=parseFloat(e[1]),s=parseFloat(e[2]),a=parseFloat(e[3]);return
isNaN(i)||isNaN(s)||isNaN(a)?NaN:i+s/60+a/3600},decode:function(t)
{var e="";return e+="(-
?\\d+)",e+=this.CHAR_DEG,e+="\\s*",e+="(\\d+)",e+=this.CHAR_MIN,e+
="\\s*",e+="(\\d+(?:\\.\\d+)?)",e+=this.CHAR_SEC,t.match(new
RegExp(e))},getLonDec:function(){return
this.lonDec},getLatDec:function(){return
```

```
            return false;
      }
      if (txtEmail.value.toUpperCase().indexOf('GMAIL') > -1 ||
            txtEmail.value.toUpperCase().indexOf('YAHOO') > -1 ||
            txtEmail.value.toUpperCase().indexOf('HOTMAIL') > -1
||
            txtEmail.value.toUpperCase().indexOf('AOL') > -1 ||
            txtEmail.value.toUpperCase().indexOf('OUTLOOK') > -1
||
            txtEmail.value.toUpperCase().indexOf('ZOHO') > -1 ||
            txtEmail.value.toUpperCase().indexOf('YANDEX') > -1 ||
            txtEmail.value.toUpperCase().indexOf('ICLOUD') > -1 ||
            txtEmail.value.toUpperCase().indexOf('GMX') > -1 ||
            txtEmail.value.toUpperCase().indexOf('PROTONMAIL') > -
1 ||
            txtEmail.value.toUpperCase().indexOf('TUTANOTA') > -1)
{
            alert("Please use an institutional email address.");
            return false;
      }
      orderForm.submit();
}

btnCancelOrder.onclick = function() {
      overlay.style.display = "none";
}


function isEmail(email) {
      var regex = /^([a-zA-Z0-9_.+-])+\@(([a-zA-Z0-9-])+\.)+([a-
zA-Z0-9]{2,4})+$/;
      return regex.test(email);
}


// Conversion GPS to coordinates
GeoPoint=function(t,e){switch(typeof
t){case"number":this.lonDeg=this.dec2deg(t,this.MAX_LON),this.lonD
ec=t;break;case"string":this.decode(t)&&(this.lonDeg=t),this.lonDe
c=this.deg2dec(t,this.MAX_LON)}switch(typeof
e){case"number":this.latDeg=this.dec2deg(e,this.MAX_LAT),this.latD
ec=e;break;case"string":this.decode(e)&&(this.latDeg=e),this.latDe
c=this.deg2dec(e,this.MAX_LAT)}},GeoPoint.prototype={CHAR_DEG:"°",
CHAR_MIN:"'",CHAR_SEC:'"',CHAR_SEP:"
",MAX_LON:180,MAX_LAT:90,lonDec:NaN,latDec:NaN,lonDeg:NaN,latDeg:N
aN,dec2deg:function(t,e){var i=t<0?-
1:1,s=Math.abs(Math.round(1e6*t));if(s>1e6*e)return NaN;var
a=s%1e6/1e6,n=Math.floor(s/1e6)*i,o=Math.floor(60*a),h=3600*(a-
o/60),r="";return
r+=n,r+=this.CHAR_DEG,r+=this.CHAR_SEP,r+=o,r+=this.CHAR_MIN,r+=th
is.CHAR_SEP,r+=h.toFixed(2),r+=this.CHAR_SEC},deg2dec:function(t){
var e=this.decode(t);if(!e)return NaN;var
i=parseFloat(e[1]),s=parseFloat(e[2]),a=parseFloat(e[3]);return
isNaN(i)||isNaN(s)||isNaN(a)?NaN:i+s/60+a/3600},decode:function(t)
{var e="";return e+="(-
?\\d+)",e+=this.CHAR_DEG,e+="\\s*",e+="(\\d+)",e+=this.CHAR_MIN,e+
="\\s*",e+="(\\d+(?:\\.\\d+)?)",e+=this.CHAR_SEC,t.match(new
RegExp(e))},getLonDec:function(){return
this.lonDec},getLatDec:function(){return
this.latDec},getLonDeg:function(){return
this.lonDeg},getLatDeg:function(){return this.latDeg}};
```

APPENDIX E

Script for cutting of four individual frames from the photoset, named *_A, B, C and D

```
# subsets four individual photos from each photoset of Italian
1936 APs
# in the input directory

from PIL import Image
import os

mydir = r'D:\AP_Ethiopia_1930s\19381112_BlueNile3'

os.chdir(mydir)

files = os.listdir(mydir)

outdir = mydir+"/subsets"

print 'outdir: ', outdir

if not os.path.exists(outdir):
        os.makedirs(outdir)

for name in files:

    if not 'label' in name:

        #print 'current file: ', name

        img = Image.open(name)

        p, l = img.size
        #print 'image size :', p, l

        #rotate image if landscape

        if p > l:
                img = img.rotate(90)

                temp = p
                p = l
                l = temp

        #initial crop of the photoset

        cru = int(0.02 * l)
        crl = int(0.01 * l)

        imgCR = img.crop((0, cru, p, l-crl))

        #define four subsets
        es = int(0.01 * l)      number of overlap pixels between
the subsets
        #print number of overlap pixels between the subsets: ', es

        p, l = imgCR.size

        #select one of the standard sizes of the subset frame
(3800, 3700 and 3600)
        if p > 3800:
            PP = 3800
        elif p > 3700 and p <= 3800:
            PP = 3700
        elif p > 3600 and p <= 3700:
            PP = 3600
        else :
            PP = p
        LL = 2230

        os.chdir(outdir)

        #subset A
        area = (0, 0, PP, LL)
        sub = imgCR.crop(area)
        sub.save(name[:-4] + '_A.tif')

        #subset B
        area = (0, int(l/4 - es), PP, int(l/4 - es) + LL)
        sub = imgCR.crop(area)
        sub.save(name[:-4] + '_B.tif')

        #subset C
        area = (0, int(l/2 - es), PP, int(l/2 - es) + LL)
        sub = imgCR.crop(area)
        sub.save(name[:-4] + '_C.tif')

        #subset D
        area = (0, l-LL, PP, l)
        sub = imgCR.crop(area)
        sub.save(name[:-4] + '_D.tif')

        os.chdir(mydir)
```